

Department of Computer Science

University of Exeter

A Tunable Measure of 3D Compactness

Submitted by

Quentin Robert Jean-Michel Lambert

to the University of Exeter as a thesis for the degree of

Master of Science by Research in Computer Science

In October 2013

This thesis is available for Library use on the understanding that it is copyright material and that no quotation from the thesis may be published without proper acknowledgement.

I certify that all material in this thesis which is not my own work has been identified and that no material has previously been submitted and approved for the award of a degree by this or any other University.

Signature:.....

Abstract

The field of shape description can be applied in domains ranging from medicine to engineering. Defining new metrics may allow to better describe shapes. It is therefore an essential process of development of the field. In this work, a new family of compactness metrics is introduced. It is proven that they range over $(0, 1]$ and are translation, rotation and scaling independent. The sphere is the shape that has the smallest volume for a fixed surface, this is a definition of compactness. Therefore, the metrics of this family are called compactness measures since they all reach 1 if and only if the considered shape is a sphere. The different metrics of the family are obtained by the modification of a parameter β involved in the mathematical definition of the metric. They are proven to be different from each other and a thorough study of their behaviour resulted in the formulation of two interesting conjectures concerning the limit cases of β . Finally several experiments investigate how McGill's database classes of shapes are represented when using the new family.

Contents

| | |
|---|-----------|
| 1 Acknowledgements | 9 |
| 2 Introduction | 10 |
| 3 Shape description and applications | 15 |
| 3.1 Definitions | 15 |
| 3.2 Literature Review | 18 |
| 3.2.1 2D Metrics | 18 |
| 3.2.2 3D Metrics | 21 |
| 3.3 Defining a new family of metric | 26 |
| 4 Theory | 28 |
| 4.1 A tunable compactness measure for 3D shapes | 28 |
| 5 Experiments | 36 |
| 5.1 Experiments | 36 |
| 5.1.1 Comparison between theory and implementation (Experiment #1) | 41 |
| 5.1.2 Differentiation between deformed shapes (Experiment #2) | 43 |
| 5.1.3 Improving classification by using several metrics (Experiment #3) | 48 |
| 5.1.4 Illustration of the different notion of compactness (Experiment #4) | 51 |
| 5.1.5 Matching experiment (Experiment #5) | 56 |

| | | |
|----------|---|-----------|
| 5.1.6 | Investigation of the class clusterisation (Experiment #6) . . . | 74 |
| 5.2 | Compactness and cubeness (Experiment #7) | 79 |
| 6 | Discussion | 81 |
| 6.1 | Approximation and proof of implementation | 81 |
| 6.2 | Database | 84 |
| 6.3 | Non-redundancy of the metric | 86 |
| 6.4 | Human perception and metric behaviour | 87 |
| 6.5 | Conjectures | 89 |
| 6.6 | The metrics in a more general context | 91 |
| 7 | Conclusion | 92 |
| A | Proof of Theorem 3 (d) | 93 |
| B | Implementation of the compactness measure | 96 |

List of Figures

| | | |
|---|--|----|
| 1 | Example of 2D shapes | 11 |
| 2 | Diagram illustrating the experimental process. | 40 |
| 3 | The set of shapes considered for the second experiment. This experiment aims at illustrating the impact of deformation on the metric values. | 45 |
| 4 | On the left, the maximum and minimum difference between two compactness measurements as a function of beta. On the right the highest and the lowest value as a function of beta. | 47 |
| 5 | Diagram illustrating a case where B1 is found closest to A1, B1 and A1 belonging to different classes, but the five closest shapes to A1 belong to the same class as A1. | 69 |
| 6 | Standard deviation as a function of the index of coherence. | 76 |
| 7 | Example of shapes to consider to realise the proof. | 91 |

List of Tables

| | | |
|----|--|----|
| 1 | Table summarizing the presented metrics. | 26 |
| 2 | Repartition of McGill's database classes between articulated and non-articulated. | 37 |
| 3 | Difference between the theoretical calculation and the numerical value obtain with the implementation of the metrics in Matlab. | 43 |
| 4 | The measured compactness for the shapes displayed in Figure 3 and for different values of β | 45 |
| 5 | The ordering resulting from the values displayed in Table 4. The compactness measurement increases from left to right. | 46 |
| 6 | Comparison between five classifiers, the four firsts use only one metric defined by a value of β whereas the last one combines the four metrics. | 50 |
| 7 | The shapes giving the 5 highest and lowest values for different values of β . The compactness increases from left to right. | 52 |
| 8 | The 10 selected shapes. | 56 |
| 9 | Matching experiment results. The first column is the shape to match, the second is the closest shapes. | 59 |
| 10 | The results that could have been expected from a human. | 60 |
| 11 | A set of results randomly generated. | 62 |
| 12 | Summary of the result obtained in this experiment, it reports the classes of the retrieved shapes. | 66 |
| 13 | The index of coherence and the standard deviation for of each class. | 76 |

- 14 Comparison between seven classifiers, the four firsts use only one metric of compactness or cubeness. The next 2 classifiers are based on the combination of two of the previous metrics chosen to be of the same type whereas the last one is the result of the combination between compactness and cubeness metrics. 80

1 Acknowledgements

This work was made possible by the funding provided by Bordeaux Graduate School of Engineering (ENSEIRB-Matmecca) and the Aquitaine region.

I would also like to thank, my supervisor Dr. Jovisa Zunic who guided me and gave me ideas for the development of this reasearch project, particularly in the theoretical results and the experiments from Section 4 and, Prof. Richard Everson and Dr. Carlos Martinez-Ortiz who gave me a lot of valuable advices.

I should also thank Katrina Dring and my parents for their support and help during this year.

2 Introduction

Progress in the field of shape description, that is the specification of metric measuring shape properties [25, 32], could benefit a number of fields, such as the fields of information processing and computational chemistry. It would make it possible to create performant search engine for 3D shapes. That is, applications that would look for shapes similar to the one given as a request. The creation would not need human intervention to fill in keywords describing the shapes. In the context of engineering and design, it would help the users retrieve past design or available components. Another approach would be to create search engines based on the submission of a similar shape. In this case a 3D sketch should be made and the program would then retrieve any similar shapes. The engineers or the designers would only need to see if the retrieved shapes fit their needs, without having to skim through the entire database. Shape description could also benefit computational chemistry given how molecule interactions is related to their shape [9, 31, 13].

The term shape in this thesis means the representation of an object in 2D or 3D. In 2D, for instance, the classical format of a shape is a black and white picture as shown in Figure 1. The 3D shape representation will be introduced in section 3. The goal of shape description is to capture specific aspects of the shapes. The aspects of a shape can be straightforward characteristics such as elongation, rectilinearity or compactness; they can also be salient or specific features of a shape, in face recognition an example would be the presence of eyes. These examples have the positive property to be easily identifiable by humans.

Other aspects can however represent shape properties that the human perception can not grasp. In a context of a fully automated application, working with purely mathematical shape descriptors may not pose any problem. In the context of human operated database, however, it is necessary that the shape descriptors correspond to aspects identifiable by human perception.



Figure 1: Example of 2D shapes

A shape descriptor can be a numeric value between 0 and 1, evaluating a specific aspect of a shape. It is worth mentioning that the merit of a descriptor greatly depends on the context of application. One extremely challenging question in computer vision is how to deal with occlusion. That is, how to describe or recognise when some of it is not visible. An example of occlusion is a car passing behind a bush, depending on the bush. Therefore finding shape descriptors that are defined even when occlusion occurs is of interest to the field. Other applications, search engines for instance, do not necessarily need to cope with occlusion and in that context it can be acceptable to work with descriptors that are not defined in a context of occlusion. Another aspect to keep in mind is the computation time, typically an application such as a search engine will need to use metrics computable in a very short time. It would not be practical to have to wait several minutes for a shape to be described, and the request on the database to be processed. In other contexts, cancer diagnosis for instance, it is admissible to use

techniques that need several hours of computation.

Another challenging problem is the ability to cope with deformation. A typical example is the posture modification of an articulated object. The various postures of a human shape can be considered deformation. If the descriptors prioritize the general shape over the small features, they are likely to be significantly dependent on any deformation. In some applications you could end up classifying dogs and cats together because they are four-legged animals. Therefore it is important to develop techniques that are deformation-independent.

For the field to fully benefit from the research on shape descriptors, it is important to assess if the newly introduced metrics are not redundant with the ones previously defined. Redundant metrics are metrics that capture the same shape aspects. A way to assess the redundancy of a set of metric is to see if the ranking deduced from the metric value over a set of shapes differs depending on the descriptor. If it does then the metrics are not redundant, if it does not and the set seem representative of the landscape of shapes then the metric can be considered redundant. By definition, it is not interesting to use redundant metrics in an application. Therefore, special care should be given to avoid introducing redundant descriptors.

A way to easily introduce new metrics is to modify a previously defined measure and make it tunable. The concept of tuning involves a variable that can be changed to modify the metric behaviour. For instance, a 2D metric could be used to compare a shape to a circle of same surface area. A way of tuning this metric could be to introduce a variable. The user would then be able to compare

the shape, not only with a circle, but also with certain ellipses. Here, the variable would represent the ratio of the two axes of the ellipse. Note that it is not sufficient to multiply the final result of a descriptor by a tunable parameter to introduce new metrics. Indeed, the transformation being linear the resulting family of metrics will be redundant. That is, changing the parameter value will not change the ranking of the shapes with regards to their metric value.

This research introduces a new family of compactness metrics. The mathematical definition of the metric is an extension to 3D of the circularity metric for 2D shapes defined in [35]. In fact it modifies the compactness metric described in [33] in a similar fashion as proposed for the 2D circularity metric. Section 3 defines several technical terms and introduces some knowledge of the field essential to understanding the contents of this research. It also reports the state of the art research of this field. The first part of Section 4 will give the theoretical definition of the metrics as well as the proof of its properties. The second part reports the experimental work realised to better understand the metrics' behaviour. Finally, Section 6 discusses and interprets the experimental results. It also points towards further interesting research. The aim of this thesis is to specify a new family of descriptors. Enriching the landscape of descriptors offers application developers a greater choice of metric to select amongst. If these metrics are proven non-redundant, it is also likely to improve the overall performance of classification applications. Shape description is a domain of image processing offering numerous application possibilities. The data collected through shape description can be used for applications such as classification model [20] or shape retrieval

[8, 17, 16]. Therefore, the validating experiment of this research will consist of such applications.

3 Shape description and applications

3.1 Definitions

There are different ways of representing shapes in a computer. These representations usually do not take colours into consideration since they rarely represent shape related information. In 2D a black and white photograph of an object can be considered a shape. A non-white pixel would be considered part of the shape. Another possible way of representing a shape is to use a polygonal approximation [14]. This consists of a set of line segments drawing the contour of a shape. It is possible to change from one representation to the other. Note however, that this change may involve a loss of precision and can be computationally expensive. In 3D, one possibility is to represent a shape with voxels. They are cubic units of space and the representation is built in a similar way as 2D shapes with pixels. That is, the space is divided into cubes, if the original shape fills more than half of a cube then the whole cube is considered belonging to the shape [12]. Another way is to use meshes [29], in this representation the original shape is sampled at a number of points. The points are then linked together usually to form a triangle mesh. This is analogous to the polygonal approximation for 2D shapes, but in a 3D context.

In most applications the data that is being dealt with is a set of shapes divided into classes. That is each shape is considered belonging to one and only one class. Examples of class can be cups, teddybears or crabs. Every shape in these classes will share similarities. Shape descriptors evaluate certain aspects

of a shape and return a certain value. Usually, several descriptors are used, consequently each shape is represented by a set of features. Using such a set of descriptors to represent shapes, results in the mapping of each shape in a space where the coordinates are the descriptor values. If the descriptors are relevant to describe a particular database, the shapes belonging to the same class will find themselves mapped near each other. It is then possible to build a model of each class [6, 30, 10]. That is, a representation based on spatial proximity.

The concept of classification will be mentioned several times in this thesis. A classification application, or classifier, consists of using a set of data to create a model able to find the class of any new shape. A set of training examples are used to create a model of the classes relevant to the application. Each example is represented by a set of measurements. In a medical context, they could be measurements such as the body temperature and the blood pressure. In the context of shape description, shape descriptors are used to describe the shapes. One of the experiments uses a nearest centroid classifier [5, 15], this particular approach to classification, consists of computing the mean value of each classes. The prediction is then made by evaluating to which class mean the new piece of data is closest. This obviously is a particularly naive approach to make predictions since being close to the class centroid is not a sufficient condition to ensure the belonging to that class. Although it does not inform on the expectable performance of an application using this metric, it allows to compare the difference in performance between classifiers. If a dataset is not large enough it can be difficult to compare classifiers because of the lack of robustness of the classification

rate. A solution to solve this problem is to use cross-validation, which consists of dividing the test set in several parts, training the classifier using all but one of them and computing the classification rate on the part left out. This process is then repeated for each part. When the dataset is too small, this technique offers an accurate comparison between classifiers, even though the results cannot be considered a fair evaluation of classifiers' performance.

This thesis aims at introducing a new family of compactness measures. The notion of compactness understood by humans usually represents the sphere as the most compact shape. Moreover, hollowed shapes, that is shapes having empty space below their surface, would be considered less compact than filled sphere-like shapes having an irregular surface. Since objects sharing a similar compactness seems to have similar shapes, studying compactness metric could lead to interesting outcomes in classification tasks. It could be argued that considering the sphere as the most compact shape is only a matter of which norm is used. Indeed, there exist mathematical definitions that would justify considering a cube as the most compact shape, the infinite norm is one of them. In this thesis a tunable formula will be introduced, its tuning parameter is added in the formula of a 3D Hu-invariant. The ordering resulting from the different tunings will be considered to define a specific notion of compactness that will differ from the classic definition.

3.2 Literature Review

3.2.1 2D Metrics

Time Complexity Shape description methods have been extensively studied for 2D shapes. In [35] the authors introduce a measure of circularity based on a Hu invariant, Zunic circularity. The time complexity of the metric for a manageable approximation can be as low as $O(r)$, where r is the image resolution. The authors of [23] introduce a convexity measure, Rahtu convexity, by interpreting the gray-scale of an image as a probability of belonging to the shape. The metric is shown to be computationally cheap, it is linear with regards to the number of pixel. The elongation descriptor, Stojmenovic elongation, introduced in [27] is based on a polygonal approximation of 2D shapes. This allows a good compromise between precision and computation time. In [34] a new measure of orientability for 2D shapes is described, Zunic orientability. Once again the computation time is said to be of linear complexity. The paper [24] proves the redundancy of a significant number of papers describing 2D roundness measurement by showing that they derive from the same formula. It is also shown that they are resolution-dependent. The two new non-redundant resolution independent metrics, Ritter roundness metrics, they introduce are proven to have linear complexity. Given the low time complexity of all these metrics, they could be a good choice for applications where time is an issue. As mentioned earlier, they could prove themselves useful in the context of a search engine.

Human Perception The authors of [35, 27] both mention that Zunic circularity and Stojmenovic elongation are close to the human perception. [24] also addresses this problem. It specifies whether or not each of the studied metric fits human perception. In particular, both Ritter roundness metrics are said to be close to the human perception of roundness. This is a desirable property in that it qualifies such metric in application involving human manipulation. The interface of a search engine could ask the user to evaluate different aspects of a shape to be found. It is essential in this sort of contexts that the metrics and the human perception agree. Although [34] does not specify whether Zunic orientability fits human perception. Orientability being a property measuring whether the shape is constructed along a specific axis. It is mentioned that the orientability of shapes plays an important role in the human visual system. A good orientability metric could help adapt the set of shape descriptors depending on the orientability of the shape.

Tuning and Redundancy In [35], Zunic circularity is extended to be tunable. Some experiments show how the tuning changes the metric behaviour, that is how the ordering of the shapes according the metric value is modified by a different tuning. It is also shown how using several tunings may lead to an improvement of performance in classification applications. It is mentioned in [23] that Rahtu convexity could be tuned by considering different thresholds for the interpretation of the gray-scale. The paper, however, lacks an illustration or a proof that this tuning would alter the metric behaviour. Although it is not tunable, in [34], Zunic orientability is explicitly shown to be non-redundant with the other measures of

orientability.

Occlusion It is worth noting that the measurements mentioned in [23, 24, 27, 34, 35], namely Rahtu convexity, Ritter roundness, Stojmenovic elongation, Zunic orientability and Zunic circularity, impose that a complete model of the shape is available. The results in the case of occlusion would be meaningless, since it must be applied to the complete model. It is also worth noting that in certain applications, occlusion-robust techniques are essential. For instance, when trying to classify objects in a scene.

Review and Further Work The authors of [25] published an extensive description and comparison of 2D descriptors. The experiments used for comparison in this article may help users choose an adapted set of features. This study is a significant piece of work as the state of the art in 2D shape descriptors. It is specified that the performance of a given metric greatly depend on the dataset on which it is used. That is the impact of the metric in increasing the rate of a classification application, for instance, depends on the data.

Further experiments could be made to better the understanding of certain metrics. For instance, a classification study of Stojmenovic elongation metric introduced in [27] could provide useful information about how it completes other metrics. It would also be interesting to explicitly investigate the redundancy of the metrics, as was done in [24]. Being able to prove the redundancy of certain descriptors would reduce the landscape of metrics available today. Making the knowledge gained by numerous studies more practical to use by decreasing the

number to investigate.

From 2D to 3D The field of research has started investigating metrics for 3D shapes. The authors of [23] pointed out that Rahtu convexity could easily be extended to 3D, by considering voxels instead of pixels. Stojmenovic elongation is based on rotating the considered shape to find an angle minimizing or maximizing the projection on the associated vector. Therefore, extending it to 3D is likely to be difficult since rotations are a lot more complex than in 2D. Similarly, nothing is said in [34] concerning the possibility of extending Zunic orientability to 3D shapes. But for similar reasons as for Stojmenovic elongation a study could reveal that the computation time increases so much that a new low complexity algorithm would need to be formulated before it is practical to use. The authors of [3] introduce two analogous metrics for 2D and 3D shapes. This compactness measure is based on the discretisation of the shapes, namely pixels and voxels for 2D and 3D respectively. They improve a previously introduced definition by allowing a computation on fragmented and porous objects. It is worth mentioning that these metrics are not able to differentiate between differently scattered compound shapes, that is, it can't differentiate between two spheres separated by 5cm and 5m. The computation time is, however, improved compared to their last work.

3.2.2 3D Metrics

Time [2] describes a discrete compactness measure, Bribiesca compactness, based on the division of a shape into multiple polyhedra. This is not a strong

constraint since certain digitisation methods are based on this principle. The voxelisation is a particular case of such a division which makes the computations straightforward. When dealing with meshes however, this technique involves a prior treatment to subdivide the mesh into tetrahedron. Thus increasing the computation time. The authors of [33] introduce a measure of compactness, Zunic compactness, for 3D shapes based on a 3D Hu moment invariant. It is also mentioned that techniques can help reduce the computational complexity to make it competitive. In [21] the authors introduce a metric that compare a shape to a cube, Martinez-Ortiz cubeness. Its computation time is linear with respect to the shape resolution. This measure is extended in [22] by adding tunability, Martinez-Ortiz tunable cubeness, and keeps its computationally cheap property. Several experiments are also run to illustrate the behaviour of the metric. A new family of geometric descriptors is introduced in [28]. It is based on asymmetry detection, Sukno asymmetry detection. The computation time is showed to be $O(r^5)$ with regards to the size of the sampling. Even if the accuracy seems to be slightly less competitive than for the other techniques, improving it may result in a performant family of metrics. These descriptors are likely to be relevant in real-time applications. The authors of [19] describe a measure of rectilinearity for 3D shapes, Lian rectilinearity. It is pointed out that the technique would benefit from further improvements to speed up the computation time and become competitive. Note that, a thorough study of the measure performance in different contexts of application is given.

Human Perception [19] references studies that suggest that the human perception seems to be strongly based on rectilinearity measurements, this justify the definition of Lian rectilinearity. Bribiesca compactness measure described in [2] agrees with human perception to the extent that a stick will be less compact than a cube. It is, however, worth noting that the most compact shape considering this metric is a cube rather than a sphere. This result is partly due to the discretisation of the shape and the resulting definition of compactness. Some experiments of [33] suggests that Zunic compactness fits the human perception. In [21] and [22] nothing is said on this subject. It may be an interesting question for future research.

Tuning and Redundancy The paper [22] also proves that using a combination of different tuning of Martinez-Ortiz tunable cubeness can lead to better results when used in a matching application. Thus, it is proven that the tuning changes the ordering of the shape according to their measurement. Although no tuning is involved, the experiments shown in [33] prove that Zunic compactness is not redundant with previously defined compactness measures.

Occlusion and Drawbacks For most of these techniques, once again, the computation in cases of occlusion is not defined. For Sukno asymmetry detection metric, [28], however, particular care was taken to obtain non-occluded data. The reason is that the technique being based on asymmetry detection, any occlusion would likely have a dramatic effect.

As a drawback for Bribiesca compactness measure, [2], it is worth noting that

it can only be applied to watertight shapes, that is whose surface define a single volume. Indeed this technique cannot differentiate between identical compound shapes scattered differently. Once again, this fact may or may not be of importance depending on the application and the dataset.

Application and Review Techniques have been developed to offer solutions to the deformation problem. It consists of finding a canonical form for the deformed shape. That is, computing a non-deformed version of the shape. In 2D, [1], introduces a method to compute an averaged shape. Even if it is not explicitly presented as a canonical form the results can certainly be used as such. Moreover the approach seems to be extendable to 3D shapes. Unfortunately, the computation time is not explicitly mentioned. The study presented in [7] aims at computing the canonical form of different 3D shapes. The experimental results show that shapes obtained via deformation of the same original shape are found to have the same canonical form, but the small features specific to each shapes are lost. The paper [18], however, introduces a method to compute the shape canonical form without losing these features. The method is computationally expensive but its results are visually impressive and should encourage further improvement and optimization.

A new dataset is also introduced in [18]. It allows to benchmark the ability of an algorithm to differentiate between classes of similarly articulated shapes, like cats and dogs for instance. Given that the individual features are lost in the metric introduced in [7], it would be interesting to see how well the technique performs on this new benchmark.

In [4] a method to describe partial 3D shapes is introduced. It is divided in a first step of feature selection and second that compares the features of different shapes and decides if the shapes are similar. The authors of [8] describe a method to realise 3D shape retrieval and recognition based on an hypergraph. It offers a method in the case where the 3D models of the shapes are not available and only views of the object are available. Thus the expensive process of rebuilding the 3D objects from the 2D views is avoided. The displayed experiments of [4], reveal classification rate of 92.44% which is a good result when compared with the other techniques. Lower quality results should however, be expected from an application in a real-world context because of choices made to speed up the computation. Similarly, the performance displayed in [8] are better than the other studied techniques but the computation cost of the process may disqualify the technique in many cases.

It is worth noting that the technique presented in [4] is extremely dependent on the kind of shapes considered, shapes with very few salient features would be difficult to identify. The technique from [8] also suffers a major drawback. It is not yet possible to update the database without recomputing the entire hypergraph. Consequently, in its actual state the method does not seem to be practical but further improvement may make it competitive. In future work, a performance study on occluded shapes may reveal itself interesting. The method introduced in [4] was designed to perform well in the case of occlusion by learning the salient features of a shape , offering a solution to one of the most challenging problem of computer vision.

| Metrics | Reference | Time | Human perception | Occlusion |
|---------------------------------|-----------|----------|------------------|-----------------|
| Zunic circularity | [35] | $O(r)$ | close | undefined |
| Rahtu convexity | [23] | $O(r)$ | not mentioned | undefined |
| Stojmenovic elongation | [27] | $O(n)$ | close | undefined |
| Zunic orientability | [34] | $O(r)$ | not mentioned | undefined |
| Ritter roundness | [24] | $O(r)$ | close | undefined |
| Bribiesca compactness | [2] | $O(r)$ | close | undefined |
| Zunic compactness | [33] | $O(r)$ | close | undefined |
| Martinez-Ortiz cubeness | [21] | $O(r)$ | not mentioned | undefined |
| Martinez-Ortiz tunable cubeness | [22] | $O(r)$ | not mentioned | undefined |
| Sukno asymmetry detection | [28] | $O(r^5)$ | not mentioned | not competitive |
| Lian rectilinearity | [19] | unknown | close | undefined |

Table 1: Table summarizing the presented metrics.

In [17] a new non-rigid 3D shape benchmark is proposed. A study of several retrieval algorithms is done using the benchmark. It is pointed out that the field could benefit from large and diverse, as well as specific benchmarks. The database proposed in [17] is based on several well-known benchmark and adds new kind of shapes to the ones previously available. This benchmark should be considered in future work. It seems to be a promising alternative to McGill's because the different classes are more balanced and thus avoid a consequent bias.

where r is the resolution of the shape and n is the number of triangle or segment depending on the shape representation.

3.3 Defining a new family of metric

Table 3.2.2 summarizes the characteristics of the presented metrics. This review showed how it is possible to formalise new metrics by extending previous definition. Indeed, this process was used to define Martinez-Ortiz tunable cube-

ness, [22], from Martinez-Ortiz cubeness [21]. Zunic compactness defined in [33] could go through a similar process. Studying compactness is relevant since it is expected that similarly compact objects seem to have similar shapes. In this research we will answer the following questions. How to extend Zunic compactness? What are the formal properties of the new family of metrics? Is the family redundant? What are the most/least compact shapes for different metrics of the family? Are they able to help increase the classification rate of a classification application?

4 Theory

This section is a theoretical work defining the new family of metrics. It also proves properties essential for a shape descriptor, as well as others specific to this family of metrics behaviour.

4.1 A tunable compactness measure for 3D shapes

The new family of metrics is based on the compactness metric introduced in [33]. In this paper, it is proven that the metric is ranging over $(0, 1]$, is invariant with regards to translation, rotation and scaling and equal to one if and only if the shape is a sphere. Note that the exact value 0 is never reached. Similarly, in [35], the extension of Zunic circularity is proven to tend towards 0 when the parameter tends toward ∞ . This subsection will focus on establishing a similar theoretical basis for the definition of the new compactness measures. Theorems 1 and 2 will establish bounds of a formula originally inspired by a Hu-invariant [11].

Theorems 1 and 2 prove what is the lower bound of $\frac{\iiint_S (x^2 + y^2 + z^2)^\beta dx dy dz}{V(S)^{(2\beta+3)/3}}$ and also establish that it is reached only in the case of a sphere. Let us consider the centroid of a shape to be its center of gravity.

Theorem 1. *Let S be a shape whose centroid coincides with the origin, β real number such that $\beta > 0$ and $V(S)$ the volume of the shape. Then:*

$$\frac{\iiint_S (x^2 + y^2 + z^2)^\beta dx dy dz}{V(S)^{(2\beta+3)/3}} \geq \frac{3}{2\beta + 3} \left(\frac{3}{4\pi} \right)^{2\beta/3} \quad (1)$$

$$\frac{\iiint_S (x^2 + y^2 + z^2)^\beta dx dy dz}{V(S)^{(2\beta+3)/3}} = \frac{3}{2\beta + 3} \left(\frac{3}{4\pi} \right)^{2\beta/3} \Leftrightarrow S \text{ is a sphere} \quad (2)$$

Proof. Consider the sphere S_p having the same volume as S and whose centroid coincides with the origin. Thus its radius r is such that $r = \sqrt[3]{3V(S)/4\pi}$. Let's consider a real number $\beta > 0$ then:

$$(u, v, w) \in S \setminus S_p, (x, y, z) \in S_p \setminus S \Rightarrow (u^2 + v^2 + w^2)^\beta > (x^2 + y^2 + z^2)^\beta,$$

which gives:

$$\iiint_{S \setminus S_p} (x^2 + y^2 + z^2)^\beta dx dy dz \geq \iiint_{S_p \setminus S} (x^2 + y^2 + z^2)^\beta dx dy dz \quad (3)$$

and by extending the integration to the intersection of both shapes:

$$\iiint_S (x^2 + y^2 + z^2)^\beta dx dy dz \geq \iiint_{S_p} (x^2 + y^2 + z^2)^\beta dx dy dz$$

and

$$\begin{aligned} & \iiint_{S_p} (x^2 + y^2 + z^2)^\beta dx dy dz \\ &= \int_{\theta=0}^{2\pi} \int_{\phi=0}^{\pi} \int_{\rho=0}^r ((\rho \cos \theta \sin \phi)^2 + (\rho \sin \theta \sin \phi)^2 + (\rho \cos \phi)^2)^\beta \rho^2 \sin \phi d\theta d\phi d\rho \\ &= \frac{3}{2\beta + 3} \left(\frac{3}{4\pi}\right)^{2\beta/3} V(S)^{(2\beta+3)/3}. \end{aligned}$$

This proves 1. To prove 2, it is enough to notice that:

- If S is not a sphere then the inequality 3 is strict, implying that 1 is also strict - i.e. 2 does not hold.

- If S is a sphere then the verification of 2 is straightforward.

□

Theorem 1 assumes $\beta > 0$ but the convergence of the integral is preserved for $-\frac{3}{2} < \beta < 0$. Moreover the reasoning stays valid except that the inequality is opposed. This leads to the next theorem, given without proof.

Theorem 2. *Let a shape S whose centroid coincides with the origin, and a constant β , such that $-\frac{3}{2} < \beta < 0$. Then:*

$$\frac{\iiint_S (x^2 + y^2 + z^2)^\beta dx dy dz}{V(S)^{(2\beta+3)/3}} \leq \frac{3}{2\beta+3} \left(\frac{3}{4\pi}\right)^{2\beta/3}$$

$$\frac{\iiint_S (x^2 + y^2 + z^2)^\beta dx dy dz}{V(S)^{(2\beta+3)/3}} = \frac{3}{2\beta+3} \left(\frac{3}{4\pi}\right)^{2\beta/3} \Leftrightarrow S \text{ is a sphere}$$

The statements of the Theorem 1 and Theorem 2 leads to the definition of a tunable 3D compactness measure.

The next definition defines the family of compactness measures by adapting the previous formula such that the new metrics range over $(0, 1]$.

Definition 1. *Let S be a shape whose centroid coincides with the origin, and a constant $\beta > -\frac{3}{2}$ such that $\beta \neq 0$. Then the compactness measure $\mathcal{K}_\beta(S)$ is defined as:*

$$\mathcal{K}_\beta(S) = \begin{cases} \frac{3}{2\beta+3} \left(\frac{3}{4\pi}\right)^{2\beta/3} \frac{V(S)^{(2\beta+3)/3}}{\iiint_S (x^2+y^2+z^2)^\beta dx dy dz}, & \beta > 0 \\ \frac{2\beta+3}{3} \left(\frac{4\pi}{3}\right)^{2\beta/3} \frac{\iiint_S (x^2+y^2+z^2)^\beta dx dy dz}{V(S)^{(2\beta+3)/3}}, & -\frac{3}{2} < \beta < 0. \end{cases} \quad (4)$$

Note that by construction, the new compactness measures $\mathcal{K}_\beta(S)$ range over $(0, 1]$ as is expected from such a descriptor. Moreover, the metric is continuous with regards to β in 0, since both formulae are equal to 1 when β is equal to 0. The reason why the metric in the case of $\beta = 0$ was chosen to be left undefined is because in this case the compactness of every shape is worth 1. It is also worth noting that the impact of β weight the points depending on their position inside the shape. It is not clear however what value of β is associated with higher weight for the points close to the center of gravity, for instance.

The next theorem summarises desirable properties of $\mathcal{K}_\beta(S)$ measure.

Theorem 3. *The new compactness measure $\mathcal{K}_\beta(S)$, where $\beta > -\frac{3}{2}$ and $\beta \neq 0$, satisfies the following properties:*

(a) $\mathcal{K}_\beta(S) \in (0, 1]$ for all shapes S ;

(b) $\mathcal{K}_\beta(S) = 1 \Leftrightarrow S$ is a sphere;

(c) $\mathcal{K}_\beta(S)$ is invariant with respect to the translation, rotation and scaling transformations;

(d) For each $\delta > 0$ and fixed β there is a shape S such that $0 < \mathcal{K}_\beta(S) < \delta$

Proof. By definition of $\mathcal{K}_\beta(S)$, (a), (b) and its invariance with respect to translation are true. Moreover, since the sub-integral $\iiint_S (x^2 + y^2 + z^2) dx dy dz$ is invariant with respect to rotation, the new compactness measure also have this property, since the shape center of gravity coincides with the origin and no other part of the metric formula could be dependent on the shape rotation. As for the

scaling invariant, it is sufficient to note that, in the case of a scaling of ratio r , the substitution $\{x \rightarrow rx; y \rightarrow ry; z \rightarrow rz\}$ in $\iiint_S (x^2 + y^2 + z^2)^\beta dx dy dz$ gives:

$$\iiint_S ((rx)^2 + (ry)^2 + (rz)^2)^\beta r^3 dx dy dz = \iiint_S r^{2\beta+3} (x^2 + y^2 + z^2)^\beta dx dy dz \quad (5)$$

$$= r^{2\beta+3} \iiint_S (x^2 + y^2 + z^2)^\beta dx dy dz \quad (6)$$

The volume resulting from such a scaling will be: $r^3 V(S)$. Consequently, the scaling related factors from the integral and the volume will cancel each other out.

The proof of (d) is obtained by considering the hollow sphere S_a , for $a \geq 1$, such that $S_a = \{(x, y, z) \in \mathbb{R}^3 \mid a \leq (x^2 + y^2 + z^2) \leq a + 1\}$. Then for every β , $\lim_{a \rightarrow \infty} \mathcal{K}_\beta(S_a) = 0$.

The details can be found in the appendix A.

□

Theorem 4. *Let S be a shape different from a sphere. Then:*

$$\lim_{\beta \rightarrow \infty} \mathcal{K}_\beta(S) = 0. \quad (7)$$

Proof. Let a shape S , different from a sphere, whose centroid coincides with the origin. Consider a sphere S_p having the same volume as S and whose centroid also coincides with the origin. Thus its radius r is such that $r = \sqrt[3]{3V(S)/4\pi}$. A consequence of this definition is that the volume of $S \setminus S_p$ and $S_p \setminus S$ are equal and strictly positive, since both shapes are centered on the origin. Hence Δ can be

defined as follow:

$$\Delta = V(S \setminus S_p) = V(S_p \setminus S) > 0 \quad (8)$$

Further, let another sphere S_{ext} centered at the origin and having a radius r_{ext} such that

$$r_{ext} = \sqrt[3]{3(V(S) + \Delta)/4\pi}. \text{ Note that } r < r_{ext} \text{ and}$$

$$V(S_{ext} \setminus S_p) = \Delta. \quad (9)$$

Similarly to the proof of Theorem 1 :

$$(u, v, w) \in S \setminus S_{ext}, (x, y, z) \in S_{ext} \setminus S \Rightarrow (u^2 + v^2 + w^2)^\beta > (x^2 + y^2 + z^2)^\beta,$$

which gives:

$$\iiint_{S \setminus S_{ext}} (x^2 + y^2 + z^2)^\beta dx dy dz \geq \iiint_{S_{ext} \setminus S} (x^2 + y^2 + z^2)^\beta dx dy dz$$

and by extending the integration over $(S \cap S_{ext}) \setminus S_p$:

$$\iiint_{S \setminus S_p} (x^2 + y^2 + z^2)^\beta dx dy dz \geq \iiint_{S_{ext} \setminus S_p} (x^2 + y^2 + z^2)^\beta dx dy dz \quad (10)$$

where

$$\begin{aligned}
& \iiint_{S_{ext} \setminus S_p} (x^2 + y^2 + z^2)^\beta dx dy dz \\
&= \int_{\theta=0}^{2\pi} \int_{\phi=0}^{\pi} \int_{\rho=r}^{r_{ext}} ((\rho \cos \theta \sin \phi)^2 + (\rho \sin \theta \sin \phi)^2 + (\rho \cos \phi)^2)^\beta \rho^2 \sin \phi d\theta d\phi d\rho \\
&= \frac{4\pi}{2\beta + 3} (r_{ext}^{2\beta+3} - r^{2\beta+3}) \\
&= \frac{4\pi}{2\beta + 3} \left(\left(\frac{3(V(S) + \Delta)}{4\pi} \right)^{(2\beta+3)/3} - \left(\frac{3V(S)}{4\pi} \right)^{(2\beta+3)/3} \right) \\
&= \frac{4\pi}{2\beta + 3} \left(\frac{3}{4\pi} \right)^{2\beta/3} \cdot V(S)^{(2\beta+3)/3} \cdot \left(\left(1 + \frac{\Delta}{V(S)} \right)^{(2\beta+3)} - 1 \right).
\end{aligned}$$

A Taylor expansion together with the fact that $\Delta < V(S)$ imply that there is an $\omega \in (0, 1)$ such that:

$$\begin{aligned}
& \iiint_{S_{ext} \setminus S_p} (x^2 + y^2 + z^2)^\beta dx dy dz \\
&= \frac{4\pi}{2\beta + 3} \left(\frac{3}{4\pi} \right)^{2\beta/3} \cdot V(S)^{(2\beta+3)/3} \\
&\quad \left(\frac{2\beta + 3}{3} \frac{\Delta}{V(S)} + \frac{2\beta + 3}{3} \frac{2\beta}{3} \frac{\Delta^2}{V(S)^2} \left(1 + \omega \frac{\Delta}{V(S)} \right)^{(2\beta-3)/3} \right) \\
&> \frac{4\pi}{2\beta + 3} \left(\frac{3}{4\pi} \right)^{2\beta/3} \cdot V(S)^{(2\beta+3)/3} \cdot \frac{2\beta + 3}{3} \frac{\Delta}{V(S)}
\end{aligned} \tag{11}$$

Thus deriving from (10) and (11):

$$\begin{aligned}
& \iiint_S (x^2 + y^2 + z^2)^\beta dx dy dz \geq \iiint_{S \setminus S_p} (x^2 + y^2 + z^2)^\beta dx dy dz \\
&> \frac{4\pi}{2\beta + 3} \left(\frac{3}{4\pi} \right)^{2\beta/3} \cdot V(S)^{(2\beta+3)/3} \cdot \frac{2\beta + 3}{3} \frac{\Delta}{V(S)}.
\end{aligned}$$

Finally,

$$\mathcal{K}_\beta(S) = \frac{4\pi}{2\beta + 3} \left(\frac{3}{4\pi} \right)^{2\beta/3} \cdot \frac{V(S)^{(2\beta+3)/3}}{\iiint_S (x^2 + y^2 + z^2)^\beta dx dy dz} < \frac{3V(S)}{3(2\beta + 3)\Delta}. \quad (12)$$

Since $\Delta > 0$ and since Δ does not depend on β , 12 gives:

$$\lim_{\beta \rightarrow \infty} \mathcal{K}_\beta(S) = 0.$$

□

Hence the Theorem 4 has been proven for every shape S different from a sphere.

One consequence of this theorem is that no matter how small is a shape difference from a perfect sphere, there is a β such that the metric, $\mathcal{K}_\beta(S)$ is able to distinguish between them. Indeed, for all δ such that $0 < \delta < 1$, there is a value of β such that the difference between a sphere and the measured shape is greater than δ .

In this section a new tunable compactness measure was introduced theoretically. It extends Zunic compactness, [33], by introducing a parameter to its definition, some of its formal properties were proven. Namely, the metrics range over $(0, 1]$, 0 being the lower bound. For any β different from 0, the compactness is equal to 1 if and only if the shape is a perfect sphere. This property is coherent with human perception, indeed it is expected that the most compact shape is a sphere. It is also invariant with regards to translation, rotation and scaling. These

are highly desirable properties, indeed as a result, the compactness value will not be dependent on how the model is presented. That is, the metrics do not differentiate between, for instance, a “view” from behind and one from above. Finally, the last theorem proves that, the measurement for any shape differing from a sphere will tend toward 0 as β increases. Consequently, it is possible to use this metric to evaluate the difference between a sphere and the measured shape.

5 Experiments

This section presents a set of experiments that illustrates the relation between the metric values and the shapes and proves its non-redundancy. Finally in the last subsection, the combined use of the new metrics and the cubeness metrics, described in [22], is studied as an example of application of the new metric in association with a previously defined metric.

5.1 Experiments

In this section, experiments are provided to answer whether the different metric of the family are redundant, what are the most and least compact shapes depending on the tuning and whether the new tunable compactness measure can increase the classification rate of an application.

McGill’s dataset is used for the following experiments, it is a commonly used dataset [26]. There are 457 shapes belonging to 19 classes. The list of the classes is: Ants, Crabs, Glasses, Hands, Humans, Octopuses, Pliers, Snakes, Spiders,

| Non-Articulated | Articulated |
|------------------------|--------------------|
| Airplanes | Crabs |
| Birds | Hands |
| Dinosaurs | Octopuses |
| Fishes | Snakes |
| Chairs | Spiders |
| Cups | Teddy-bears |
| Dolphins | Ants |
| Four-limbed | Humans |
| Tables | Pliers |
| | Glasses |

Table 2: Repartition of McGill’s database classes between articulated and non-articulated.

Teddy-bears, Tables, Cups, Chairs, Airplanes, Dolphins, Birds, Four-legged, Dinosaurs and Fishes. The classes themselves are divided into two kinds, objects with articulating parts and objects without, Table 2 shows the repartition. Every class of the non-articulated kind, is composed of essentially different objects. For instance the class “Table” does not contain twice the same table. For the classes belonging to the articulated kind, it is worth noting that most shapes of every class are obtained by deformation of an initial shape. Typically, in the case of the crab class, every shape was obtained by changing the posture of the crab legs. The number of shapes in each class varies from 12 to 31 shapes. As pointed out in [17], the unequal repartition of shapes among the different classes may cause a bias. Since we will be evaluating the relative classification rate rather than their numerical value, McGill’s dataset remains a satisfying choice.

The different experiments were realised with the software Matlab. Using the “.im” version of the shape in the database. Appendix B gives the code used to compute the measurement for a shape from the shape file. It defines the function

`Kbeta` that takes a file name and a parameter *beta* and returns the compactness value of the shape stored in the file for the parameter value *beta*. `Kbeta` expects the filename to point to a file representing a shape in the format “.im”, the loading function, namely `kuim_load`, import the shape as a matrix of voxels. A procedure then called this function for every shape of the database and for 10 different values of β . These values were chosen to cover a range of values within the limit of the metric computability. The different values of β are: -1.4, -1, -0.5, -0.1, 0.1, 0.5, 1, 2, 3. These will be enough to prove the non-redundancy and show an increase in classification rate, it will also be possible to illustrate the difference between the most and least compact shapes for various tunings. The compactness measurements were stored to be post-processed later in the different experiments.

The formula defining the compactness metric is based on the integration of the term $(x^2 + y^2 + z^2)^\beta$ over the considered shape. In this work, this integral is approximated by dividing the shape into “unit” of space and considering the formula constant over this volume. The constant value of each “unit” of space is chosen to be the value of the formula for its center of gravity. Each voxel was subdivided into a sufficient number of cubes to obtain a satisfying precision. It is important to specify that a voxel is unit of space with regards to the shape representation but it is still possible to subdivide it mathematically. Note that, for every β greater than 0, $(x^2 + y^2 + z^2)^\beta$ is defined in $(0, 0, 0)$. Consequently, the integration converges rapidly, meaning that it is not necessary to consider an extremely fine precision to reach a satisfying approximation. However when β is lower than 0, $(x^2 + y^2 + z^2)^\beta$ becomes $\frac{1}{(x^2+y^2+z^2)^{-|\beta|}}$, which is not defined in

$(0, 0, 0)$, but $\iiint_S \frac{1}{(x^2+y^2+z^2)^{-|\beta|}}$ still converges, if $-1.5 < \beta < 0$. This implies that as β tends toward -1.5 a much finer precision is needed to obtain an accurate result. The consequence of these remarks from the point of view of the code was that for positive value of β it is sufficient to subdivide each voxel into 4 cubes to obtain satisfying results. The code shown in Appendix B, however, displays a subdivision into 1000 cubes, it was used to compute the measurements for negative values of β . As mentioned previously, the measurements were originally computed for 10 values of β . The numerical values of the metric obtained for certain shapes in the case of $\beta = -1.4$ revealed themselves to be higher than 1. This is due to the fact that the chosen approximation was not fine enough. It was decided not to use it and run the experiments using only nine different values of β . It is important to note that the choice of the sample size, that is the number of successive subdivision of the voxels, has an important impact on the computation time. Indeed, the computation were a matter of seconds for positive values of β , whereas it took an average of 15 minutes to compute the four negative values of β for each shape. Consequently, for the metric to be practical in the context of negative values of β a significant improvement of the computation method is needed. This improvement is left for future work.

Figure 2 displays an illustration of the experimental process. The experiment reported in Section 5.1.1, comparison between theory and implementation, gives evidence to justify the correct implementation of the algorithm by comparing several theoretical results to the ones obtained by computation. That is it is an attempt at giving piece of evidence that the implementation actually compute the

metric value. The following experiment, “named behaviour on a set of deformed shape”, detailed in Section 5.1.2, investigate the ability to differentiate amongst a set of deformed shape. In Section 5.1.3 the experiment, improving classification by using several metrics, investigates how the use of the new family of metrics can lead to an improvement in classification. These two experiments will give valuable results to draw a conclusion on the non-redundancy of the metrics. In Section 5.1.4, the illustration of the different notions of compactness gives a graphic overview of the different compactness definitions described by the metric tunings. Section 5.1.5 reports the results of a matching experiment which gives a graphic illustration of the metric ability to describe a dataset. Finally, the investigation of the class clusterisation, in Section 5.1.6, attempts to better understand the previous results by illustrating how the classes of McGill’s database are mapped by the metrics.

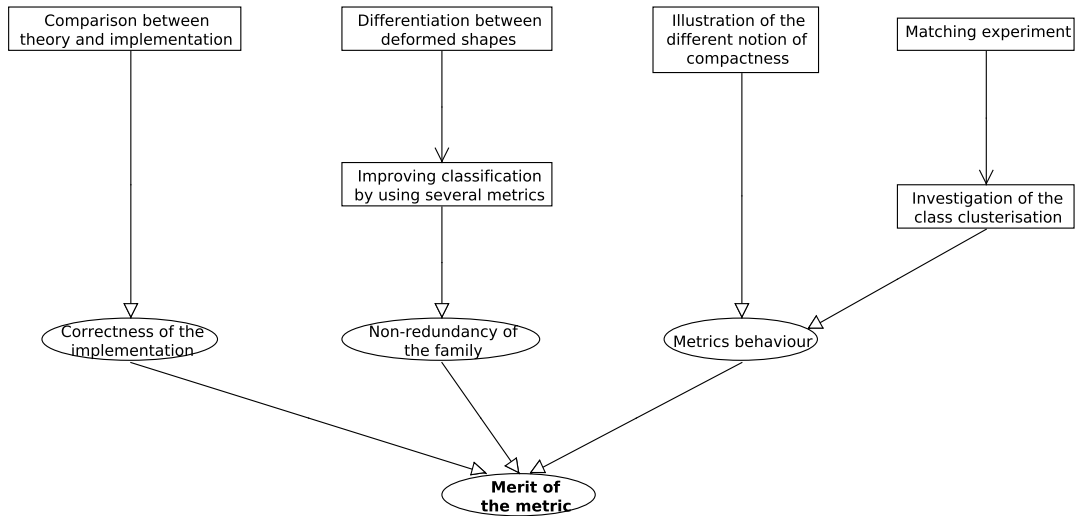


Figure 2: Diagram illustrating the experimental process.

5.1.1 Comparison between theory and implementation (Experiment #1)

In this subsection, theoretical calculation of the compactness of a cube for three different values of β , namely 1, 2 and 3, will be compared with the results from the implemented version of the computation. These values were chosen because they were the only results obtainable through a hand written theoretical calculation. This experiment is an attempt to justify the correctness of the metric implementation and thus the relevance the data that will be used in subsequent experiments. The calculation for $\beta = 3$ will be fully detailed. Given the similarity of reasoning the values for the other β will be given without further justifications.

Let C be a cube centered on the origin and of volume 1. Since:

$$\mathcal{K}_\beta(C) = \frac{3}{2\beta + 3} \left(\frac{3}{4\pi} \right)^{2\beta/3} \frac{\mu_{0,0,0}(C)^{(2\beta+3)/3}}{\iiint_C (x^2 + y^2 + z^2)^\beta dx dy dz}$$

Then:

$$K_3(C) = \frac{3}{9} \left(\frac{3}{4\pi} \right)^2 \frac{1}{\iiint_C (x^2 + y^2 + z^2)^3 dx dy dz}$$

The integral gives:

$$\begin{aligned}
 & \iiint_C (x^2 + y^2 + z^2)^3 dx dy dz \\
 &= \iiint_C x^6 + 3x^4(y^2 + z^2) + 3x^2(y^2 + z^2)^2 + (y^2 + z^2)^3 dx dy dz \\
 &= \iiint_C x^6 + 3x^4y^2 + 3x^4z^2 + 3x^2y^4 + 3x^2z^4 + 6x^2y^2z^2 + y^6 + z^6 + 3y^4z^2 + 3y^2z^4 dx dy dz
 \end{aligned}$$

Since it is integrated over the same intervals, it is possible to rename the variables to obtain:

$$\begin{aligned}
 &= \iiint_C 3x^6 + 18x^4y^2 + 6x^2y^2z^2 dx dy dz \\
 &= \int_{x=-0.5}^{0.5} \int_{y=-0.5}^{0.5} \int_{z=-0.5}^{0.5} 3x^6 + 18x^4y^2 + 6x^2y^2z^2 dx dy dz \\
 &= \int_{x=-0.5}^{0.5} 3x^6 dx + \int_{x=-0.5}^{0.5} \int_{y=-0.5}^{0.5} 18x^4y^2 dx dy + \int_{x=-0.5}^{0.5} \int_{y=-0.5}^{0.5} \int_{z=-0.5}^{0.5} 6x^2y^2z^2 dx dy dz \\
 &= \frac{6}{7}0.5^7 + \frac{72}{15}0.5^8 + \frac{48}{27}0.5^9
 \end{aligned}$$

Finally:

$$\begin{aligned}
 \mathcal{K}_3(C) &= \frac{3}{9} \left(\frac{3}{4\pi} \right)^2 \frac{1}{\frac{6}{7}0.5^7 + \frac{72}{15}0.5^8 + \frac{48}{27}0.5^9} \\
 &\approx 0.6569
 \end{aligned}$$

Table 3 gives the difference between the theoretical calculation and the result of the computer assisted computation. For the three values, the order of magnitude of the difference is 10^{-5} . These results are low enough to be confident about the correctness of the implementation, if it wasn't the case the measure would have

likely resulted in a very different value. Since the computation on a cube are not as complicated as on the shape of McGill's database any results lower than $2.5e - 03$ will be considered not precise enough given the current implementation. The way we proceeded to determine how much we had to subdivide the voxels, was by successively increasing the level of subdivision. Eventually, the computation time for the metric reached a level where we wouldn't have been to compute the data. $2.5e - 03$ is greater than the highest value difference between the two last step of the process. That is, the greatest difference between the results obtained when subdividing each cube into 729 cubes and those obtained for a subdivision into 1000 cubes, was lower than $2.5e - 03$. Note that this value is also higher than the difference found between theoretical calculation and numerical computation.

| β | Difference value |
|---------|------------------|
| 1 | $1.4093e - 05$ |
| 2 | $3.2194e - 05$ |
| 3 | $4.8025e - 05$ |

Table 3: Difference between the theoretical calculation and the numerical value obtain with the implementation of the metrics in Matlab.

Conclusion The results obtained in this section gives us confidence that our implementation correct, it also gave us the opportunity to evaluate the margin of error that is being made with our implementation, namely $2.5e - 03$.

5.1.2 Differentiation between deformed shapes (Experiment #2)

This experiment aims at illustrating how close the metrics value of a set of shapes obtained by deformation are from each other. Figure 3 shows the set of shapes

considered for this experiment and Table 4 their compactness measurements for different values of β .

The data used in this experiment is composed of 5 shapes. Each shape was obtained by deformation of an initial teddy-bear (Figure 3 teddy10). The different shapes are in fact different postures of this teddy-bear.

In order to accept that the metric can differentiate between this set of shapes, the measurement difference between any two shapes should be higher than the error margin fixed in the previous experiment, namely 0.0025. The reason for that is that any result based on a difference of value lower than this threshold could potentially be proven wrong by a more precise approach. Consequently if the mean value is found to be lower than 0.0025, the value of β to which it corresponds will be disqualified in future experiment.

This experiment is also an opportunity to assess the redundancy of the metric. A sufficient condition to prove that it is not redundant is to observe a difference in the ranking of the shapes according to their compactness measurements for different values of β . This is not a necessary condition because the dataset is not representative of every shape. Consequently, although the ordering might not change on this dataset, it might be possible to observe a modification with a more representative one.

Table 5 shows the ordering resulting from the numerical value. Finally, Figure 4 displays the lowest compactness measure for the set and the lowest difference between two shapes as a function of β . The plot also displays the threshold representing the error margin.

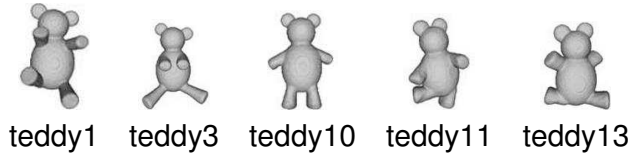


Figure 3: The set of shapes considered for the second experiment. This experiment aims at illustrating the impact of deformation on the metric values.

| β | -1 | -0.5 | -0.1 | 0.1 | 0.5 |
|---------|------------|------------|------------|------------|------------|
| teddy1 | 8.8788e-01 | 8.8672e-01 | 9.6670e-01 | 9.6210e-01 | 7.8758e-01 |
| teddy3 | 9.0323e-01 | 8.9108e-01 | 9.6598e-01 | 9.6011e-01 | 7.6684e-01 |
| teddy10 | 8.9450e-01 | 8.9293e-01 | 9.6871e-01 | 9.6449e-01 | 8.0141e-01 |
| teddy11 | 9.0202e-01 | 8.9725e-01 | 9.6923e-01 | 9.6461e-01 | 7.9712e-01 |
| teddy13 | 8.9820e-01 | 8.9583e-01 | 9.6946e-01 | 9.6524e-01 | 8.0406e-01 |

| β | 1 | 2 | 3 | 6 |
|---------|------------|------------|------------|------------|
| teddy1 | 5.5963e-01 | 2.2496e-01 | 7.4346e-02 | 1.5399e-03 |
| teddy3 | 5.0711e-01 | 1.6006e-01 | 4.0043e-02 | 4.0406e-04 |
| teddy10 | 5.8802e-01 | 2.6426e-01 | 1.0234e-01 | 3.6021e-03 |
| teddy11 | 5.7071e-01 | 2.3018e-01 | 7.6237e-02 | 1.6853e-03 |
| teddy13 | 5.8991e-01 | 2.6067e-01 | 9.7428e-02 | 3.0857e-03 |

Table 4: The measured compactness for the shapes displayed in Figure 3 and for different values of β .

The results obtained for $\beta = -0.1$ and $\beta = 0.1$ are close to 1. From the theoretical analysis of the formula, it can be deduced that the compactness measurement of each shape tends towards 1 when β tends toward 0. Moreover, Figure 4 right plot illustrates this behaviour, indeed it is clear that when β tends towards 0 the lowest and the highest compactness value of the set tends toward 1. Note also that the two rows corresponding to these values of β in Table 5 are identical. This may suggest that the two metrics behave in a similar way.

In the case of $\beta = 0.5$ and $\beta = 2$ the lowest difference between two shapes is higher than the threshold, as shown Figure 4 left plot. Consequently, these two metrics would qualify to differentiate between the different elements of this set of shapes.

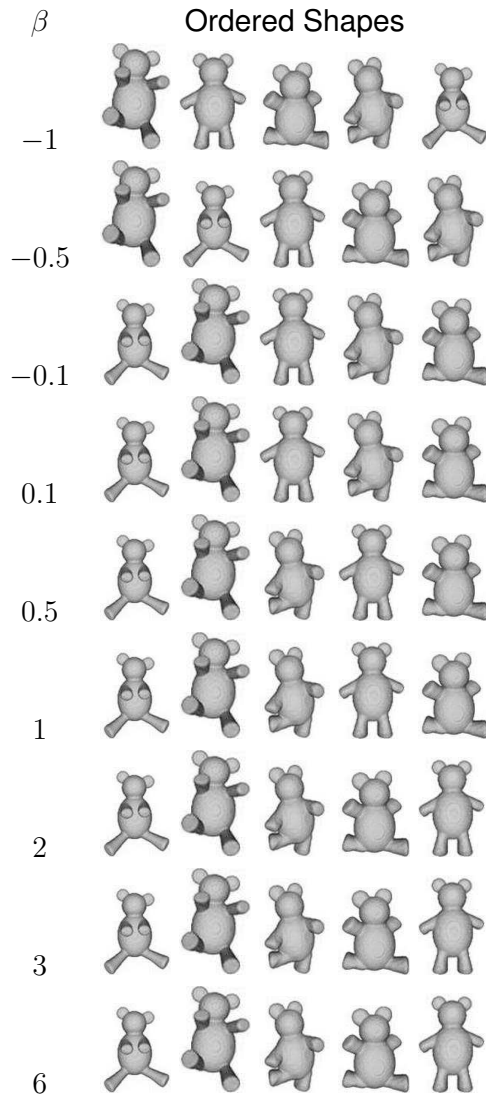


Table 5: The ordering resulting from the values displayed in Table 4. The compactness measurement increases from left to right.

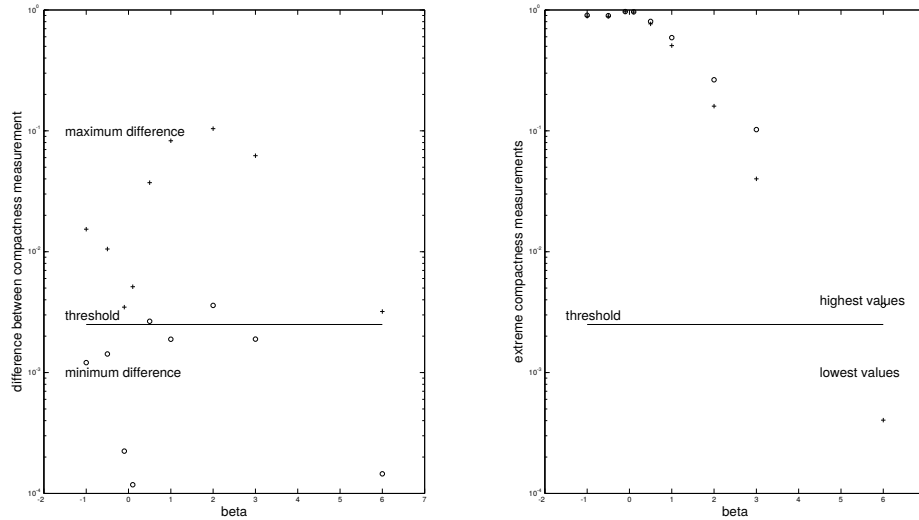


Figure 4: On the left, the maximum and minimum difference between two compactness measurements as a function of beta. On the right the highest and the lowest value as a function of beta.

Figure 4 left plot clearly shows that the minimum difference obtained for $\beta = 0.1$, $\beta = -0.1$ and $\beta = 6$ are significantly below the threshold of the error margin for this research. It means that the relative ranking can not be relied on. More importantly, in the case of $\beta = 6$, Figure 4 right plot shows that the lowest compactness measurements is below the threshold. Consequently it is safer to take it away from further experiments, since it can not be relied on.

It is also worth noting that the lowest difference for $\beta = 3$, $\beta = 1$, $\beta = -0.5$ and $\beta = -1$ are shown to be notably close to the threshold in Figure 4 left plot. Consequently, an improvement in the precision of the metric could result in accepting these metrics as able to differentiate between the shapes of this dataset. Moreover Table 5 shows that the shape ordering for these four metrics are different. It suggests that a combined use would result in an improvement of performance for a shape description application. This hypothesis will be further studied in the

experiment #3, improving classification by using several metrics. As mentioned earlier, the change of ordering observed in this part brings evidence that the family of metrics is not redundant.

Conclusion This experiment investigated the ability of a single metric to differentiate amongst the member of a particularly small dataset. The results presented clearly show that for our implementation and according to the margin of error we chose certain tuning of the metric can appropriately differentiate between the shapes, namely, $\beta = 0.5$ and $\beta = 2$. Note that on a larger dataset it is highly unlikely to be able to differentiate between every shapes using only one metric. Therefore, it makes more sense to rely on the non-redundancy of a set of metrics to describe the shapes. Moreover, choosing an appropriate set of metrics may be enough to compensate for a lack of precision. This experiment also brings some piece of evidence that the metrics of the family are not redundant by displaying a modification of the shape ordering.

5.1.3 Improving classification by using several metrics (Experiment #3)

This experiment consists of a numerical evaluation of the performance of different classifiers based on the family of metrics.

In last experiment, it was shown that the metrics defined by $\beta = 3$, $\beta = 1$, $\beta = -0.5$ and $\beta = -1$ may not be able to differentiate between the shapes of the studied dataset, alone. It was also pointed out that the ranking that resulted from their respective compactness value was different. As a consequence it was

mentioned that a combined use may lead to an improvement of performance, in a classification application for instance.

To assess whether or not a combined use of these metrics would improve the performance of an application, five nearest-centroid classifiers were built. The choice of not using advance machine learning techniques was made in order to make sure that any performance improvement was due to the non-redundancy of the family rather than a better convergence of the classification method. Four of the five classifiers used a single metric defined by a specific value of β . These values were used as data for the classification task. The fifth classifier was obtained by training on the four previously used metrics.

The classification rate was computed by 3-fold cross-validation on the entire McGill's database. This technique allow for a fair comparison between the different classifiers.

Note that the classification task consisted of assigning a class among 19 to each shape of the test sample. From here on the classes we will be referring to are the on listed in Table 2. Consequently a random classifier would be characterised by a classification rate of 0.05. If the classifiers succeed in outperforming such a classifier, it would imply that the compactness measure are relevant in the description of certain class of McGill's dataset.

Figure 6 shows the results.

The classification rate of the classifiers using a single metric are all higher than 0.05. Moreover, the classifier built using the four metrics has a classification

| β | Classification Rate |
|----------------------|---------------------|
| $\{-1\}$ | 0.2122 |
| $\{-0.5\}$ | 0.2429 |
| $\{1\}$ | 0.2165 |
| $\{3\}$ | 0.2428 |
| $\{-1, -0.5, 1, 3\}$ | 0.3741 |

Table 6: Comparison between five classifiers, the four firsts use only one metric defined by a value of β whereas the last one combines the four metrics.

rate higher than any of the others.

The first remark that can be made concerning the results displayed in Table 6 is that the classifiers using a single metric outperform a random classifier. Thus, it can be deduced that compactness measurements are relevant in the description of the shapes of McGill's database. Experiment 5.1.6 will investigate whether certain classes are characterized by their compactness values. Indeed if every class had a great diversity of compactness, the result from the classifier would likely be worse than a random classifier. However, if the compactness was sufficient to describe every class of the dataset, a much higher rate would be expected.

The second point that can be deduced from the results is that the combined use of the metrics effectively result in a better classification performance. Indeed the table clearly shows an increase between any single classifier and the classifier using the combination of metrics. This proves that the family of metrics is not redundant. Indeed if the different tuning of the metric were all redundant the classification rates should all be equal. The fact that the classification rate doubles is an indication that the notion of compactness defined by the different tuning are relevant in the characterisation of certain classes.

Conclusion This experiment successfully brought more evidence of the non-redundancy of the family of metrics defined in this thesis. Indeed the difference of performance is an indicator of this fact. It was also shown that the classifier using a combination of metrics outperformed the classifiers using only one of them. Moreover, they all outperform a random classifier, this suggests that the notions of compactness defined by the family of metrics are relevant in the characterisation of certain classes of McGill's dataset. In a more general perspective it means that a combined use of several metric of this family can result in an improvement of performance.

5.1.4 Illustration of the different notion of compactness (Experiment #4)

This experiment gives an illustration of the most and least compact shapes for the metrics, it will show the different notions of compactness defined by the family of metrics.

The dataset used in this experiment is the entire McGill's database. It is considered to be diverse enough to accurately illustrate the various compactness definition rising from different tunings of the metric. Given the remark made in the previous experiment concerning $\beta = 6$ the results for this metric are not studied. For each value of β the shapes corresponding to the five highest and the five lowest values of the metric were selected, Table 7 displays the results.

The shapes leading to the 5 lowest values can be considered the least compact for the considered metric. Similarly, the 5 highest values are the most compact shapes. A significant change in the retrieved shapes would be an indica-











































| β | Lowest | | | | | Highest | | | | |
|---------|---|---|--|--|---|--|---|--|--|---|
| -1 |  snakes13 |  snakes14 |  glasses23 |  glasses18 |  glasses4 |  octopuses63 |  fishes16 |  octopuses26 |  octopuses25 |  cups22 |
| -0.5 |  glasses23 |  snakes13 |  snakes14 |  glasses4 |  glasses18 |  octopus26 |  octopus63 |  octopus25 |  fishes16 |  cups22 |
| -0.1 |  glasses23 |  snakes19 |  glasses4 |  glasses18 |  snakes8 |  teddy11 |  teddy13 |  teddy20 |  fishes16 |  cups22 |
| 0.1 |  snakes19 |  glasses23 |  glasses4 |  snakes8 |  snakes20 |  teddy11 |  teddy13 |  teddy20 |  fishes16 |  cups22 |
| 0.5 |  snakes20 |  snakes19 |  snakes8 |  glasses23 |  glasses4 |  teddy10 |  teddy20 |  teddy13 |  cups22 |  fishes16 |
| 1 |  snakes20 |  snakes19 |  snakes8 |  glasses23 |  glasses20 |  teddy20 |  cups22 |  teddy10 |  teddy13 |  fishes16 |
| 2 |  snakes20 |  glasses20 |  glasses3 |  snakes19 |  glasses13 |  teddy8 |  cups9 |  teddy13 |  teddy10 |  cups4 |
| 3 |  snakes20 |  glasses3 |  glasses20 |  glasses12 |  glasses1 |  cups2 |  teddy13 |  teddy10 |  cups9 |  cups4 |

Table 7: The shapes giving the 5 highest and lowest values for different values of β . The compactness increases from left to right.

tion that the metric behaviour is significantly modified as β changes. The study of these modifications and the appearance of the shapes might reveal general trends from which to formulate conjectures describing the metric behaviour.

The metric being continuous, a slight difference in the retrieved shapes for successive value of β and a significant change when considering a large difference in the value of β is expected.

For $\beta = -1$ and $\beta = -0.5$, 3 octopuses are found to be amongst the most

compact shapes of the database. All of them have a very spherical base that would qualify as a high compactness, but their tentacles should reduce their compactness value. **The metric seem to consider compact the shapes having a strong compact part around their center of gravity.** The results obtained for the least compact shapes seem to support this hypothesis. The 2 least compact shapes in the case of $\beta = -1$ are spring-like shapes. It is clear for these shapes that none of their points are close to the center of gravity. The other shapes that are considered not compact are glasses with their arms unfolded. In these cases, the center of gravity might belong to the shape but because the glasses arms are not in the same plane as the lenses it is shifted in the arms direction. In extreme cases it might be shifted enough not to belong to the shape. This would not be the case if the arms were in the same plan. All these remarks tends to confirm that the fewer point around the center of gravity, the lesser the compactness. Note that this notion is fairly different from human perception in the sense that the tentacles would likely result in classifying the octopuses as less compact than teddy-bears for instance.

Some of the results for $\beta = 2$ and $\beta = 3$ are unexpected. Indeed, empty cups are retrieved amongst the 5 most compact shapes. This suggests that as β increases the metric considered cups as being more compact than, for instance, teddy-bears. It seems that the points of the shapes far away from the center of gravity have a more significant impact than the closer ones. That is, **the metric is evaluating how close the shape is to an hollowed sphere.** The hollowed sphere is considered to be a sphere with a concentric hole. The tinier the hole

of the sphere, the more compact. This could explain why hollowed shapes are retrieved. The cups are quite spherical when looking on the opposite side of the handle. It is difficult to comment on the less compact shapes since their compactness values happen to be of the same order of magnitude as the margin error. From the conjecture the only prediction that can be made is that as β increases the less compact shapes will be the ones with the smallest volume away from their center of gravity. The retrieved shapes do not falsify the conjecture, it is however difficult to precisely evaluate such a qualitative criteria. Another hint that the conjecture might be true is that the octopuses retrieved in the case of $\beta = -1$ and $\beta = -0.5$ are down to the 150th place in the overall ranking. It is relevant because as β would increase the tentacles importance over the body is supposedly going to increase. This would result in a decrease of compactness and that is what is observed here.

In the previous experiment a remark was made considering the fact that the ordering for $\beta = 0.1$ and $\beta = -0.1$ was similar and that it could be the sign that it behaves in a similar manner. The results obtained for the most compact shapes in these cases would tend to support this remark. Indeed, the five most compact shapes are the same for both tunings. The least compact, however, are significantly different. It is, therefore, safe to say that this two tunings of the metric behave in a different manner. As mentioned previously the compactness of every shape tends toward 1 as β tends toward 0. A consequence of this fact is that the metrics are likely to loose being interesting if β is too close to 0, since the metric value for all shapes tends toward 1. This is something to keep in mind

when selecting a set of metrics. It is worth noting that the most compact shapes are coherent with the human perception. Note that the cup, which is the most compact shape is not empty. Therefore, there is no obvious difference with the human perception of compactness. Similarly, the least compact shapes are rather thin and as such agree with human expectations of a non compact shape. It could however be argued that more linear shapes should be expected. That is, a stick may be considered less compact than the displayed glasses.

The same sort of remarks holds for $\beta = 0.5$ and $\beta = 1$. That is, both the least and the most compact retrieved shapes are fairly consistent with human perception. Moreover, the results obtained for $\beta = 1$ seems to better address the remark concerning a stick-like shape. One pair of glasses is swapped in favor of another pair whose arms are in the same plan as the lenses. The general remark that the metric for $\beta = 1$ is coherent with the human perception confirms what had been said in [33]. This paper specifically studied the case where β was equal to 1. In fact, the retrieved shapes for these two metrics are very similar to the ones retrieved for $\beta = 0.1$ and $\beta = -0.1$. In particular, the results for $\beta = 0.1$, $\beta = 0.5$ and $\beta = 1$ are composed of the same shapes. This suggests that the metric behaviour does not vary very much when β belongs to $(0, 1]$.

Conclusion As was expected, a slight change can be observed between successive rows of the table. Indeed, for any two successive table rows at least two shapes can be found in both. This is coherent with the fact that the metric is continuous with regards to β . Moreover, there is at least a slight change of ordering in the retrieved shapes which is enough to confirm that the family is not redundant.

In fact, in almost every two successive rows a new shape is introduced. This illustrates that the behaviour of the metric changes significantly overall. One particularly satisfying result is that the first row and the last row of the table have no shape in common. It is satisfying because it strongly suggests that as β is changing, the aspects of the shapes that are being evaluated change dramatically. It is worth noting that the compactness metrics defined for β close to -1.5 seems to weight more the points of the shape close to its center of gravity whereas when β increases, the most important points in describing the shape compactness seem to be the points away from the center of gravity.

5.1.5 Matching experiment (Experiment #5)

In this experiment, 10 shapes were randomly chosen so that they belong to different classes. This was done as a way to give a broader illustration of the metrics. The list of shapes is shown in Table 8.











| | | | | |
|---|---|---|---|---|
|  |  |  |  |  |
| teddy5 | crabs18 | glasses1 | hands5 | octopus26 |
|  |  |  |  |  |
| airplane9 | cups22 | snakes30 | humans9 | four5 |

Table 8: The 10 selected shapes.





































For each of these shapes, the 5 closest shapes were retrieved. Where closeness refers to the smallest distance computed by considering the metric values of a shape as its coordinates. As mentioned in 3, computing the value of n different

metrics result in the mapping of each shape in an n -dimensional space. That is, each metric value is a coordinate and the shape itself can be considered to be located at the corresponding position. Consequently, the distance between two shapes is the euclidean distance. In this experiment the following values of β were used: -1, -0.5, -0.1, 0.1, 0.5, 1, 2, 3. Note that $\beta = 6$ was ruled out for the reasons mentioned in the second experiment (differentiation between deformed shapes).

Here, it is expected that a naive use of different metrics of the family will result in a satisfying shape matching application. There are different ways to assess it but the purpose of this thesis is to show the contexts in which the metrics are interesting shape descriptors rather than to build the best matching model possible. Therefore, the general aspects of the retrieved shapes will be compared with the submitted one. Strong similarities in compactness are expected, and possibly shapes of the same class. Indeed, suppose that compactness measurements of certain classes are more dependent on the kind of shapes than on the posture; it results that the most similar compactness are more easily found in the same class than in other classes. The class teddy-bear seem to be a good example of that phenomenon. To improve the assessment, two other tables of an analogous experiment are also shown. Table 10 is a personal selection, it is supposed to represent a human answer to the question: "What are the most similar shapes to the one submitted". Table 11 is a random choice of shapes in the database. This table is here to help the reader consider the difference between the retrieved shapes and a random result.

The results of this experiment could illustrate that on some database the merit of this metric is straight forward. This experiment will also give an intuition of the contexts in which the metric is a good descriptor.

Table 9 displays the results of this experiment. Note that the retrieved shapes are not ordered in any way.

| Submitted shape | Five closest shapes | | | | |
|---|---|---|---|---|---|
|  |  |  |  |  |  |
| teddy5 | teddy2 | teddy8 | teddy6 | teddy16 | teddy20 |
|  |  |  |  |  |  |
| crabs18 | crabs24 | crabs11 | crabs5 | crabs21 | crabs3 |
|  |  |  |  |  |  |
| glasses1 | snakes16 | glasses10 | glasses16 | glasses3 | glasses19 |
|  |  |  |  |  |  |
| hands5 | hands3 | crabs4 | hands8 | hands7 | crabs14 |
|  |  |  |  |  |  |
| octopuses26 | dinosaurs16 | octopuses25 | octopuses67 | octopuses7 | dinosaurs4 |
|  |  |  |  |  |  |
| airplanes9 | ants13 | airplanes8 | ants5 | airplanes17 | ants28 |

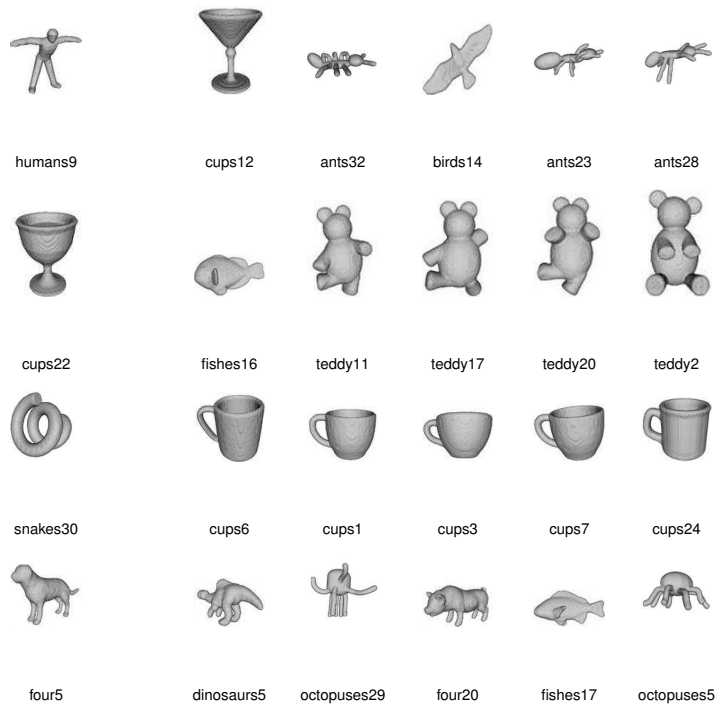
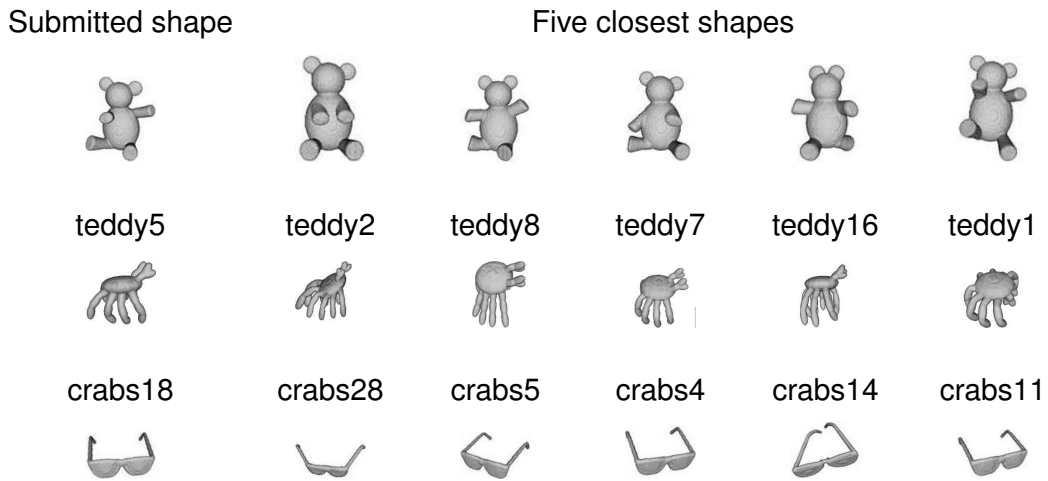


Table 9: Matching experiment results. The first column is the shape to match, the second is the closest shapes.



Submitted shape

Five closest shapes








































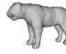



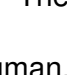




| | | | | | |
|---|---|---|---|---|---|
| glasses1 | glasses17 | glasses10 | glasses16 | glasses15 | glasses19 |
|  |  |  |  |  |  |
| hands5 | hands3 | hands9 | hands8 | hands7 | hands1 |
|  |  |  |  |  |  |
| octopu26 | octopu14 | octopu25 | octopu12 | octopu7 | octopu9 |
|  |  |  |  |  |  |
| airpla9 | airpla7 | airpla8 | airpla1 | airpla23 | airpla22 |
|  |  |  |  |  |  |
| humans9 | humans5 | humans6 | humans7 | humans8 | humans10 |
|  |  |  |  |  |  |
| cups22 | cups21 | cups16 | cups17 | cups14 | cups11 |
|  |  |  |  |  |  |
| snakes30 | snakes4 | snakes14 | snakes13 | snakes2 | snakes27 |
|  |  |  |  |  |  |
| four5 | four6 | four12 | four17 | four15 | four19 |
|  |  |  |  |  |  |

Table 10: The results that could have been expected from a human.

Submitted shape

Five closest shapes



teddy5



dinosaurs17



chairs22



tables18



cups20



glasses18



crabs18



four25



crabs9



dolphins1



humans4



tables19



glasses1



hands20



tables4



spiders29



spiders25



humans25



hands5



humans11



crabs29



cups20



humans15



crabs12



octopu26



pliers12



hands20



chairs12



ants34



tables4



airpla9



cups17



teddy7



snakes12



glasses12



airpla24



humans9



teddy16



pliers9



ants23



cups13



teddy6















| Submitted shape | Five closest shapes | | | | |
|---|---|---|---|---|---|
| cups22 | octopu51 | four9 | tables8 | chairs3 | airpla14 |
|  |  |  |  |  |  |
| snakes30 | ants34 | teddy13 | glasses4 | fishes2 | hands5 |
|  |  |  |  |  |  |
| four5 | humans24 | birds11 | snakes19 | chairs7 | airpla3 |

Table 11: A set of results randomly generated.

The human perception is extremely performant but it has a major flaw. Indeed, we evolved as a species to identify patterns. This ability is such that the human brain can even find them where there is none. For instance, when looking up and staring at clouds which are randomly shaped, it is not uncommon to recognise identifiable shapes. In an attempt to avoid this process when interpreting the results Table 11 was generated randomly. This should give the reader a fair ground to look at the results and draw accurate conclusions. The submitted shapes are the same but the retrieved ones are randomly generated. As expected from a randomly generated sample the retrieved shapes rarely belong to the class of the submitted one. It is common to observe five retrieved shapes belonging to five different classes.

Table 10 was not an attempt to evaluate which shapes have a similar compact-

ness. It was rather an illustration of what shapes a human could have considered the closest. This is personal evaluation and therefore is not representative of human choices. For the teddy-bears, the crabs, the hands, the octopuses and the humans different postures of the initial model were chosen. Whenever possible the postures that looked the most like the submitted shape were prioritised. It is worth mentioning that the selection was particularly difficult in the case of the octopuses. Evaluating similar position, when taking into consideration the eight tentacles is clearly a matter of opinion. Similarly, for the glasses, only the shapes based on the same original model were selected. Their arms being in slightly different positions. For the airplanes and the cups, the general appearance was the main criteria. Therefore in the case of the airplanes the size and shape of the wings vary slightly. For the cups, only the ones having a foot were selected. The cups having a semi-spherical shape were prioritised over the more conic ones. The snakes were only selected if they were in some kind of spiral. The row submitting a dog was the most difficult. The class it belongs to is the four legged animals. As a consequence there were virtually no similar shapes. The other dog-like animals present in the class were chosen. To fill the two remaining slots, the shapes that had a similar aspects with regard to the size of their body and legs were chosen. In every case only shapes from the same class as the submitted shape were selected.

The two first rows of Table 9 are notable because the retrieved shapes clearly belong to the same class as the submitted ones. Namely, submitting the teddy-bear resulted in the retrieval of five teddy-bears. Similarly, the five closest shapes

to the crab were found to be crabs themselves. The pair of glasses were closest to four other pairs and one snake. Among the four pairs of glasses only one of them is not based on the same original model. The hand and the octopus were associated with three shapes belonging to their respective class and two others from a different class. Namely, the hand received two crabs as an answer and the octopus two dinosaurs. It is worth noting that the two crabs are in a similar posture and similarly the two dinosaurs also look alike. The five shapes that were found the closest to the plane, are three ants and two planes. One of these two planes is notably similar, whereas the other is clearly different. The three ants have very different position but their legs only represent a small percentage of their body. The cup was associated with four bears and one fish. The snake led to the retrieval of five similar cups. The shapes retrieved in the case of the human are three ants, one cup and one bird. The cup has a foot and is conic and empty. The last row of the table shows that the dog was associated with another four legged animal, two octopuses, one fish and one dinosaur. Table 12 summarises this description by displaying the class of the retrieved shapes.

| Submitted shape | 5 closest shapes | Personal evaluation | Random |
|-----------------|------------------|---------------------|--|
| teddy5 | 5 teddy | 5 teddy | 1 dinosaur 1 chair 1 table 1 cup 1 glasses |
| crabs18 | 5 crabs | 5 crabs | 1 four |

| Submitted shape | 5 closest shapes | Personal evaluation | Random |
|-----------------|----------------------------|---------------------|--|
| | | | 1 crab |
| | | | 1 dolphin |
| | | | 1 human |
| | | | 1 table |
| glasses1 | 4 glasses 1 snake | 5 glasses | 2 spiders 1 hand 1 table 1 human |
| hands5 | 3 hands 2 crabs | 5 hands | 2 humans 2 crabs 1 cup |
| octopuses26 | 3 octopuses 2 dinosaurs | 5 octopuses | 1 plier 1 hand 1 chair 1 ant 1 table |
| airplanes9 | 2 airplanes 3 ants | 5 airplanes | 1 airplane 1 cup 1 teddy 1 snake 1 glasses |
| humans9 | 3 ants | 5 humans | 2 teddy |

| Submitted shape | 5 closest shapes | Personal evaluation | Random |
|-----------------|------------------|---------------------|-------------|
| | 1 bird | | 1 plier |
| | 1 cup | | 1 ant |
| | | | 1 cup |
| cups22 | 4 teddy | 5 cups | 1 octopus |
| | 1 fish | | 1 four |
| | | | 1 table |
| | | | 1 chair |
| | | | 1 airplanes |
| snake30 | 5 cups | 5 snakes | 1 ant |
| | | | 1 teddy |
| | | | 1 glasses |
| | | | 1 fish |
| | | | 1 hand |
| four5 | 1 four | 5 four | 1 human |
| | 2 octopuses | | 1 bird |
| | 1 fish | | 1 snake |
| | 1 dinosaur | | 1 chair |
| | | | 1 airplane |

Table 12: Summary of the result obtained in this experiment, it reports the classes of the retrieved shapes.

The results displayed in the two first rows of Table 9 are clearly coherent with human perception. Indeed the corresponding line in Table 10 is highly similar. As reported in Table 12, for both, teddy5 and crabs18, the five closest shapes belong to the same class. This suggests that the different notions of compactness defined by the family of metrics accurately describe teddy-bear like and crab like shapes. It is difficult to evaluate how well the metric describes specific postures. It can however be said that no obvious incoherence can be noted in the retrieved postures for the two first lines. When comparing these results with the random results from Table 11 it is clear that the new metrics successfully describe essential aspects of these two shapes.

The third line is slightly different from human perception. As shown in Table 12, four glasses and one snake are retrieved. Moreover, Table 9 shows that one of the pair of glasses is not based on the same model. The fact that the least compact shapes retrieved were consistently a mixture of glasses and snakes, possibly explain the retrieval of snake. This also suggests that the compactness measures defined by different tunings of the formula tend not to differentiate between glasses and snakes. That is, from the point of view of the different notions of compactness these shapes are similar. This is not necessarily an undesirable property. Although, it does not match, in a straight forward manner, human expectation, it is still possible to understand the qualities of the shape retrieved. They are rather thin and positioned on a curvy path rather than on a straight line. Obviously this criterion is very qualitative, as such it is possible that this would only be one of these patterns that humans can find. When comparing the results

with the corresponding line from the Table 11 the only retrieved shape that could fit the description would be the table. Therefore this criterion is satisfying as a description of what the metric is evaluating.

The three hands retrieved in the fourth line were among the ones selected as a personal choice example. Table 12 specifies that together with these three hands, two crabs were retrieved. Hence, the results clearly differs from human expectations. A description of the general aspects of the shapes could be a fairly compact basis with thinner parts along a single direction. That is, once again human perception seems to be able to catch the kind of shapes that would qualify as being the closest. Table 11 confirms that the criteria is restrictive enough to rule out a random choice. It is clear that the retrieved shapes have a greater uniformity than a random sample. The fact that crabs were retrieved when an hand was submitted is something that should be further investigated. Indeed it could mean that the closest shape to these crabs are not only crabs themselves. This would falsify the remark made previously concerning the fact the crabs seem to be well described by the metrics. Note that the space considered in this experiment has eight dimensions. In such a space, it is fully possible that a shape A was retrieved as the closest to a shape B, B belonging to another class, and that the five closest shapes to A belong to the same class as A. Figure 5 illustrates this phenomenon in 2D.

According to Table 12 the five closest shapes to octopuses²⁶ are three octopuses and two dinosaurs. As shown in Table 9, one of the octopuses is not part of the human selected sample. Therefore, it can be said that the results differs from

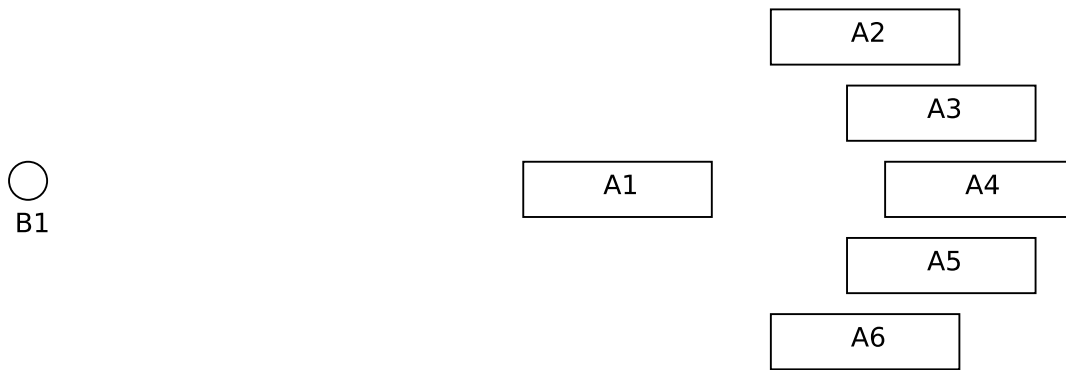


Figure 5: Diagram illustrating a case where B1 is found closest to A1, B1 and A1 belonging to different classes, but the five closest shapes to A1 belong to the same class as A1.

human perception. Admittedly, the two dinosaurs are extremely similar but it is hard to make the connection with the octopuses. One tentative explanation could be provided by the fact that the metric is rotation independent. These shapes happen to have a significant part of their volume concentrated around their center of gravity in an almost spherical manner. From this base either tentacles or an head and a tail depart. Since the metric is rotation independent and the basis almost spherical, as long as the center of gravity is left unchanged, it is possible that moving the basis of the tentacles over the surface would not significantly change the metrics values.

Applying this transformation, it seems possible to build a dinosaur-like shape out of an octopus without significantly modifying its compactness measurements. Therefore, this property could indeed account for the results. Once again comparing the result from Table 9 with the ones from Table 11, it is clear that there is a pattern between the shapes retrieved that do not fit a random selection. These results suggest that neither an hand nor an octopus are described accurately by the metric family.

The results obtained for the sixth studied shape, namely airplanes₉, are difficult to reconcile with human perception. Indeed, as reported, in Table 12, there are more ants being retrieved than airplanes and, according to Table 9, among the two retrieved planes one is clearly different from the original. Moreover the personally selected sample, displayed in Table 10, clearly shows that there were at least three planes that were notably close, from a human perception perspective at least, to the one submitted. The results for this shape clearly show that for certain set of data the family of metrics describe in this thesis are evaluating aspects of the shapes that are not coherent with human perception. When compared with the results from Table 11, the results still appear fairly uniform. A description of the retrieved shape could be a linear basis with lateral parts in the same plan. The problem with this description is that the ratio between the two components is expected to have an impact on the compactness measure. In this case, the volume involved in representing the wings and fins of the plane is clearly bigger comparatively than the one responsible for the limbs of the ants. Eventually, the only thing that can be said for certain, is that from the metric point of view ants and planes are similar. To further the understanding of the metric, it would be interesting to study the closest shapes to an ant.

The row that shows the five closest shapes to the shape, human₉, is the least consistent with human perception. As shown in Table 12, none of the closest shapes belong to the same class, indeed three ants, one bird and one cup were retrieved. There is no argument that these shapes do not agree with the selected sample found in Table 10. The fact that the shape is found to be closest to three

ants might have an interesting interpretation. Indeed the plane was also found to be close to three ants. It might be the case that ants and planes share a similar description from the metric family point of view. This remark would tend to be confirmed by the presence of a bird within the retrieved shapes. Indeed a bird shares clear shape similarities with a plane. It is however difficult to explain the presence of the cup and the human. As far as the comparison with the random results goes, it is very difficult to find a set of criteria that would describe the shapes and that would not be a random pattern. The fact that the retrieved cup is empty and has this conic shape is probably the reason of this result. The aspects of the shapes being evaluated in this case does not appear to be perceptible by humans.

Once again the retrieved shape for the full cup does not fit the human expectations. Indeed most retrieved shapes are bears and one fish is also selected. Here it is clear that the description of the cup was greatly influenced by the fact that it is full whereas the others are not. The fact that a cup is empty or not is unlikely to be relevant in a classification application unless in a very specific context. This behaviour should be kept in mind when choosing a set of metrics because it can lead to undesirable results. It is worth mentioning that the shapes that were retrieved could have been expected. Indeed these shapes are amongst the most compact shapes retrieved for $\beta \in [-0.1, 1] \setminus \{0\}$ in last experiment. It is clear that all these shapes have a similar compactness and therefore are close to each other in the context of this experiment. These results lead to another remark, classes with a great compactness disparity are less likely to be described

accurately by whatever definition of compactness is proposed. This is an obvious constation, but it nevertheless is an essential aspect to consider for someone interested in using the family of metrics. Once again as far as the random selection goes the results displayed in Table 9 are clearly uniform in the sense that they all are amongst the most compact shapes for certain values of β .

The ninth row of Table 9 displays the five shapes closest to snake30. The human expectation would be to find other snakes in the same sort of spirally position, hence the human selected results displayed in Table 10. As reported in Table 12, the algorithm found that the five closest shapes were cups. This clearly does not fit human perception but looking at the shapes of the cups it seems to make sense. In fact, when considering compactness, the results reveal an interesting behaviour of the metric family. The position of the snake is almost as if it had been rolled over the surface of a cup. That is, the space created inside the spiral could be similar to the one inside a cup. Moreover most of the shape itself appears to be concentrated in a spherical layer away from the center of gravity. This trait is shared by the cups that have been retrieved. It is certainly the reason for the observed results. The consistency in the shapes retrieved suggests a non-random behaviour. Even if it does not fit the human perception this result is very interesting to further the illustration of the metric behaviour. In this case, the layout of the shape impacts a lot on the measure of compactness, consequently the described family is not a reliable choice to describe this class. In other contexts however, it may be essential to describe shapes according to whether or not they are mainly based on a compact part. This result clearly

suggests that for such application, the described metric would be a good choice.

The final row of the table displays the results for a dog. The class this shape belongs to is the four-limbed animals. As a consequence the diversity of shape in this class is important. As mentioned earlier the human sample was selected by considering their subclass, in this case being a dog, and their general shape similarities. It is worth noting that in this case none of the shapes a human would expect is retrieved. One reason for that is something that is that the diversity of this class is such that human perception and compactness consideration do not agree. Among the shapes retrieved, there are two octopuses, one fish, one four-limbed animal and one dinosaur. This sample seem fairly random and it is difficult to find uniformity in the aspect of the sample itself. That is, not only does the shapes come from various different classes but they do not look alike. The only aspect that the human perception seem to be able to interpret could be that they all share a cylindrical part as the main component of their body. This however does not seem to be a satisfying criterion. It is probably a good example of where the metric family capture aspects that the human perception is not trained to recognise. It seems here that the metric is not adapted to describe accurately the shapes of the four-limbed class. Moreover, this example gives an illustration of a situation where the human perception can not be reconciled with the results obtained through the use of metrics.

Conclusion This experiment was using a combination of metrics in an attempt to properly describe the different shapes. The examples of the snake and the cup showed results that greatly diverge from human expectation. This illustrates

the fact that if certain classes have a great diversity of compactness amongst their shapes, the studied metric family is unlikely to succeed in describing them accurately. In the case of classes with similar compactness however, the metric seems to properly describe the different classes. The most notable examples are teddy-bears and crabs. The dog and the human examples also illustrate that the results obtained might not be interpretable by humans. Overall, it is justified to use elements of this family of metrics when some of the classes of the database have a consistent compactness. Another case where the metric could reveal itself interesting would be in a case where specific compactness related features needs to be identified. A good example of that is the case of the snake. Although retrieving cups was not what was expected from a human point of view the similarity in design might be useful to exploit. The metric could help retrieve shapes having specific layout from a database.

5.1.6 Investigation of the class clusterisation (Experiment #6)

This experiment attempts to give an insight into the results obtained in the matching experiment. It investigates the way the different classes of McGill's dataset are described by the metrics, in order to better understand their merit in matching experiments.

As mentioned in Section 3, the ability of a metric to describe a class is highly dependent on the dataset. The fifth experiment stated that some classes seemed to be accurately described by the metric. This supposition was based on the fact that the five closest shapes of one of their elements was found to belong to

the same class. It was decided to evaluate, for every shape, how many among the five closest belonged to the same class. These results were then averaged over each class to give a representation of the compactness similarities within a class to formalise an index representing a class. This number will be called index of coherence since it is an attempt to measure the coherence of a class when mapped according to their compactness measurements. Another index is studied, namely the standard deviation of the distance of each shape to the mean of their class. The point of this experiment is to give an insight of the way the class are mapped by studying these two indices. Table 13 displays the results of this experiment. Figure 6 displays the standard deviation as a function of the index of coherence.

A class will be considered well described by the family of compactness measures if in average more than four shapes among the five closest belong to this class. The standard deviation is expected to decrease as the index increases. Since that would mean that as more and more adjacent shapes are found to belong to the same class the resulting cluster tightens.

It is expected that the remark made concerning the crabs and the teddy-bears being well described by the family of metric will be confirmed by a mean higher than four. Similarly, it is expected that the four-limbed class will have a rather low result, between one and two.

The lowest value of index of coherence obtained in this experiment is 1 shape. This value is reached for the octopuses class and the birds class. That is, for ev-

| Class | Index of coherence | Standard deviation |
|-------------|--------------------|--------------------|
| Airplanes | 2.5 | 0.0191 |
| Ants | 2.5 | 0.1055 |
| Birds | 1.0 | 0.3144 |
| Chairs | 1.6 | 0.1555 |
| Crabs | 2.2 | 0.0808 |
| Cups | 2.2 | 0.2605 |
| Dinosaurs | 1.3 | 0.0140 |
| Dolphins | 1.2 | 0.0178 |
| Fishes | 1.2 | 0.0515 |
| Four-limbed | 1.8 | 0.0398 |
| Glasses | 3.4 | 0.1232 |
| Hands | 1.3 | 0.0181 |
| Humans | 2.4 | 0.1049 |
| Octopuses | 1.0 | 0.0631 |
| Pliers | 3.9 | 0.1767 |
| Snakes | 1.4 | 0.2525 |
| Spiders | 2.2 | 0.0160 |
| Tables | 1.6 | 0.1243 |
| Teddy-bears | 4.35 | 0.0058 |

Table 13: The index of coherence and the standard deviation for of each class.

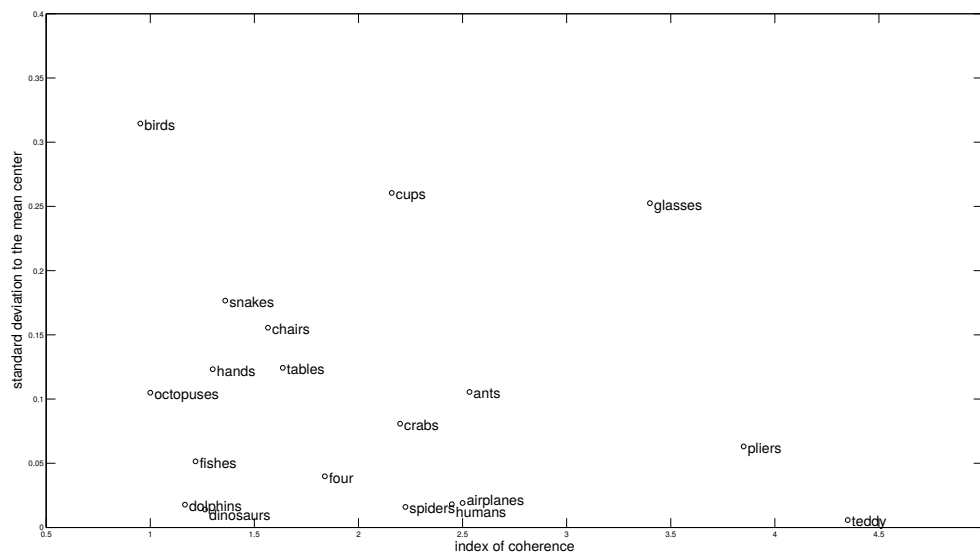


Figure 6: Standard deviation as a function of the index of coherence.

ery shape of these two classes, in average, only one shape among the five closest belong to the same class. The highest value is an average of 4.35 shapes, and is reached in the case of the teddy-bears class. Amongst the 19 classes, only five of them have an average higher than 2.5, that is, classes whose elements are found closest to, in average, 2.5 shapes of the same class.

As expected, the teddy-bears class displays an index of coherence higher than 4. Moreover, its standard deviation is the lowest which suggest a rather compact cluster. This confirms the remark made previously stating that the class was well described by the new family of metric. Indeed, if a set of metrics describes accurately a class, it is expected that the resulting mapping will lead to a cluster containing the shapes of a same class. The prediction made concerning the four-limbed animals is also confirmed, indeed it was expected to observe a coherence index between 1 and 2 and the class index is 1.8. This clearly suggests that the family of metrics does not represent accurately the class, indeed such an index suggests that in average only 2 shapes among the five closest belong to the same class for each member of the four-limbed animals. This is coherent with what was observed in the experiment reported in Section 5.1.5. The reason proposed in this part however was that this class displays a great diversity of compactness. This supposition does not agree with the standard deviation found here, namely 0.0398. The result obtained for the crabs class, however, differs from the analysis made in this subsection. Indeed, Table 13, displays an index of coherence of 2.2 for this class. Which is virtually equivalent to the one

obtained in the case of the four-limbed animals. This would mean that the results obtained in the matching experiment were not representative of the rest of the class. This confirms the doubts raised from the results found in the case of the hand in Section 5.1.5. Indeed, in this case two crabs were retrieved. The remark made in the previous paragraph, stating that only five classes among 19 have an index of coherence higher than 2.5 clearly suggests that the family of metrics is not able to describe accurately every class of the database. It is interesting to note that the standard deviation of the distance and the index of coherence have a correlation of -0.084394 . Indeed, Figure 6 shows a cloud of points rather than any sort of curve. Note in particular that good clusterisation does not guarantee a high index of coherence. Indeed if the clusters are superimposed, for instance, a small standard deviation would not be sufficient to assure a good classification performance. This phenomenon explains why the four limbed animals are not well described even though they seem to be mapped in a fairly tight cluster. That is, other shapes belonging to different classes must have a similar compactness as the shapes of the four-limbed animals.

Conclusion The only class that appears to be accurately described by the family of metrics is the teddy-bears class. It was shown that the previous remark concerning the crabs class being properly described by the metrics is wrong. The fact that only five classes have a coherence index higher than 2.5 suggests that McGill's database classes can not be described accurately by the new family of metrics alone. As expected, it is essential not to limit oneself to the use of this new family but to complete a set, based on it, with 3D shapes descriptors

capturing other shape aspects.

5.2 Compactness and cubeness (Experiment #7)

This last study aims at showing how the new metric completes a previously defined descriptor, namely Martinez-Ortiz cubeness, [22], in forming a set of descriptors for classification. This study is composed of two experiments.

The first one is similar to the third experiment (Improving classification by using several metrics), it aims at proving that a combined use from metrics belonging to these two families can result in an improvement of performance of a naive classifier. The second experiment aims at showing how the clusterisation is modified by the use of cubeness measures.

The cubeness metric described in [22] is defined by:

$$C_{\beta}(S) = \begin{cases} \frac{3}{2^{\beta}(\beta+3)} \cdot \frac{\mu_{0,0,0}(S)^{(\beta+3)/3}}{\min_{\theta, \phi \in [0, 2\pi]} \iiint_{R(S, \theta, \phi)} \max(|x|, |y|, |z|)^{\beta} dx dy dz}, & \beta > 0 \\ \frac{2^{\beta}(\beta+3)}{3} \cdot \frac{\min_{\theta, \phi \in [0, 2\pi]} \iiint_{R(S, \theta, \phi)} \max(|x|, |y|, |z|)^{\beta} dx dy dz}{\mu_{0,0,0}(S)^{(\beta+3)/3}}, & -3 < \beta < 0 \end{cases} \quad (13)$$

where $R(S, \theta, \phi)$ is the shape resulting from rotating S by θ and ϕ on the corresponding axis. Similarly as for the new compactness metrics, the cubeness metrics were proven to range over $(0, 1]$ and to be rotation, translation and scaling independent. A value of 1 is however equivalent to the shape being a cube rather than a sphere, hence the name cubeness metric.

In the classification experiment, the values of β considered for the compactness and the cubeness measures were $-1, 2$. These values are different enough

| Type of metric | β | Classification Rate |
|-----------------------|------------------------|---------------------|
| Compactness | $\{-1\}$ | 0.2210 |
| | $\{2\}$ | 0.2473 |
| Cubeness | $\{-1\}$ | 0.2560 |
| | $\{2\}$ | 0.2626 |
| Compactness | $\{-1, 2\}$ | 0.3065 |
| Cubeness | $\{-1, 2\}$ | 0.4070 |
| Compactness, Cubeness | $\{-1, 2\}, \{-1, 2\}$ | 0.4157 |

Table 14: Comparison between seven classifiers, the four firsts use only one metric of compactness or cubeness. The next 2 classifiers are based on the combination of two of the previous metrics chosen to be of the same type whereas the last one is the result of the combination between compactness and cubeness metrics.

for the resulting metrics to evaluate significantly different shape aspects [22].

Therefore, a classifier based on these cubeness measures will perform better than a classifier based on a single cubeness measure and the effect on the classification rate of the combination of cubeness measures and compactness measures will be observable. Table 14 shows the results of this experiment. In a similar manner as for experiment #3 it is expected to observe an improvement, of the classification rate, between the classifiers using the compactness measures and the one using them in combination with cubeness metrics.

Table 14 shows that the classification rate associated with the single classifiers are different from each other. The classifier based on the two compactness metrics has a classification rate higher than any of the single classifiers, it is however significantly below the one based on the cubeness measures. Finally, the classifier based on all four metrics display a slight improvement from the cubeness based one.

Conclusion The difference of result between the classifiers based on two metrics indicate that the two tunings of the cubeness metric describe McGill's database better than the chosen compactness descriptors. Moreover, the low classification rate improvement between the two last rows of the table shows that the compactness does not help much in improving the result obtained for a cubeness based classifier. That is, in the case of McGill's database, the compactness metrics do not add much information to what was obtained using cubeness metrics. It may be the case that cubeness is more suited to describe the dataset.

These results show that the compactness base classifier can be improved using cubeness metrics, although its impact on McGill's database is low. The compactness metrics may however be better suited to the description of another database.

6 Discussion

In this part, the main conclusions deduced from the experiments will be highlighted. The approach that was chosen as well as several technical aspects and further experiments will be discussed.

6.1 Approximation and proof of implementation

The shapes of McGill's database released in the ".im" are defined using voxels. It is worth noting that the voxelisation process is not rotation invariant. It can therefore result in different measurements for the same original shape. An-

other problem is that voxelisation involves a significant loss of precision. Indeed, the voxelisation process triggers a paradox. As the precision of the process increases, the volume of the representation tends toward the volume of the original model. The surface of the representation however tends toward ∞ , in a similar way as Menger sponge. This implies that it is not possible to run any surface based computation. For instance a metric whose definition is the ratio between surface and volume would not be computable. A solution to this problem would be to use a mesh representation of the shapes. Such a version of McGill's database is available in ".ply" format. Consequently, another approach was considered in an attempt to reach a better approximation. The idea was to import the shapes as triangle meshes, to divide them into tetrahedra and integrate the formula over each tetrahedron. A first version of this approach has been coded. The first attempts to use it revealed themselves far too expensive with regard to their computation time, in fact we haven't been able to compute the result for a cube. Indeed the version was coded in Octave, a clone of Matlab. Octave being python based, any code runs in average several times slower than with Matlab, whose functions are C-based. More importantly, this thesis aim is to introduce and illustrate a new metric rather than compute extremely precise values it was therefore decided to rule away this approach.

The results are computed by subdividing each voxel into cubes and approximating the formula over each of them as being the value in its center multiplied by its volume, this was chosen as a compromise between an exact value and a computation time for 35000000 voxels inferior to 90 seconds. A different approach that

might reveal itself more practical in the case of negative beta would be to integrate over each voxel rather than increase the subdivision to obtain a better precision. The computation of an integral over a cube might reveal itself quicker than over a tetrahedron and may outperform the computation time involved by too fine a sampling of each voxel. This method also has the advantage to solve another problem that arose from the implementation made to approximate the integral. Indeed, as can be seen in Appendix B, the computation were made by sampling each voxel. As mentioned earlier the precision of the calculation is greatly dependent on the size of the sampling but a sampling too great can result in a computation time for the entire database whose order of magnitude is several months. Therefore, in the cases were the integral converged quickly, namely for positive values of β , a smaller sample was used. This involved changing hard coded values in the code and resulted in computation errors, that were later solved. It was particularly unpleasant since the computation took several days and the errors could only be found by comparing them to already existent results. Therefore future work could improve the way the voxels are sampled. Such an improvement should be made so that the user would fix the size of the sample rather than hard code the sample. In that context a particular care should be taken to generate the sampling in a way that avoids any bias. In the actual version of the code a very naive approach was used. The sampling was done by subdividing the cube into smaller cubes, although the method works the computation time increases exponentially with the number of subdivision. It is not proven that such an approach is needed to obtain precise enough values.

The results obtained in the first experiment do not prove the correctness of the implementation. They merely suggest that the implementation is not grossly false. There is a whole field of computer science dedicated to the proof of correctness of programs. It involves using automatic provers. The problem of interest in this thesis being extremely mathematical, it is likely that these techniques could have given satisfying results. Unfortunately, the time did not allow to obtain this formal result. Another way to comfort our confidence in the correctness of the implementation is through the reproducibility of the numerical values. Indeed, if other research groups were to obtain the same figures for McGill's benchmark, it would increase the confidence in the results. Obviously, this approach is not practical in the context of a Master Thesis. Another, approach can be to reuse the code in other contexts. Indeed, studies in the field of software engineering suggested that reusing a piece of code in numerous application resulted in an improvement of its quality by correcting the bugs.

6.2 Database

It was suggested to use McGill's shape database to illustrate how the family of compactness measures is behaving. The original format of the shapes is the ".im" format, it seemed to have been described by the group responsible for the KUIM Image Processing System (<http://infocom.cheonan.ac.kr/nykwak/kuim/kuim.html>). Unfortunately, no open source description of the format is available which make it impossible to develop new tools. This led to the issue of importing the shapes in Matlab, it was solved thanks to Carlos Martinez-Ortiz who gave us a piece of

code based on the KUIM package. It imports the “.im” format files in the form of a matrix of voxels. Another, problem came with the visualisation of the shapes, indeed the tools available on the website seem not to have been updated since 2008 and certain libraries they use, are not standard anymore. It is mentioned on McGill’s benchmark website that their source code is to be released, unfortunately there is no way of knowing how long ago this announcement was made and if it is still to be expected. Therefore, a text file was generated from the matrix of voxels, this text file was then imported by ArtOfIllusion thanks to another of Carlos Martinez-Ortiz’s script. The software gives a 3D representation of the shapes and allows the user to easily rotate them. This process was then used to obtain the shape representation missing from the website. It also allowed to check if certain cups were empty. The field would greatly benefit from an unified open-source interface to import and interact with the shapes.

Some of the issues mentioned here may be solved by the work described in [17]. Indeed, the authors built a new benchmark of 600 watertight triangle meshes. Each shape was obtained from the deformation of 30 original models. A class consequently consist of the original shape and 19 deformed version. This allows for a reduction of the bias due to an uneven repartition of the shapes in different classes. For the purpose of this work, namely an illustration of a metric family behaviour McGill’s is sufficient. Moreover, it is a commonly used database which make it easier to compare performance of different techniques but the mentioned bias should encourage the community to move toward more recent and less biased benchmark.

6.3 Non-redundancy of the metric

The results of the second experiment (differentiation between deformed shapes) clearly showed a modification in the ordering of several tuning of the metric. This modification suggests that changing the value of β effectively changes the behaviour of the metric. That is, tuning β allows the metric to capture different aspects of the shapes.

In order to confirm the non-redundancy of the metric it is sufficient to observe a change in the classification rate. This is what has been investigated in the third experiment. As expected, the performance of the classifiers based on single metric are different from each other. Moreover the combined use increases the performance of the classifier. At least in the context of McGill's database, the different captured aspects are relevant in the description of the shapes.

These two results prove that the described family of metrics is not redundant. Moreover it illustrates the fact that a combined use of metrics can increase an application performance.

It should be reminded that the numerical value of the classification rate can not be relied on because of the small size of the test sample. Therefore it should be considered as a gross estimate. As such, it is worth noting that this value is too low for the classifier to be accepted as performant. Note that no advanced machine learning techniques were used. These techniques could increase the classification rate. Moreover, in a real-life application, it is recommended to use other metrics than the ones from the family being studied in this thesis. Indeed considering metrics that are evaluating aspects of the shapes other than their

compactness is likely to increase the performance of any application, as long as these metrics are relevant to the dataset description.

6.4 Human perception and metric behaviour

In the case of certain applications it may be important to connect the metric behaviour with the human perception. The fourth experiment, reported in Subsubsection 5.1.4, gives an illustration of the notion of compactness defined by the different values of β . The classic human perception of compactness seems to agree more with values of β close to 1. Indeed, the most compact shapes are mostly teddy-bears, the two other shapes are a full glass and a rather spherical fish. The fact that the glass is full clearly justify its high compactness measure. When β increases it was pointed out that the metric seems to be evaluating how close to an hollowed sphere is the shape. Similarly, as β tends toward -1.5 the metric seems to behave more and more like a metric that would value more the shapes having an important ratio of their volume close to their center of gravity. It is worth noting that the results of this experiment were compared with a personal selection. This was aimed at representing the human perception. This obviously induces a bias since the selection was made by a non neutral subject. Therefore, it would be interesting to gather a proper human sample and compare the resulting ordering of the shapes with the one obtained for different values of β . This would better illustrate how the metric relates to human perception. Moreover, the comparison was done using 2D representation of the 3D shapes, comparing resin models of the 3D shapes could further decrease the bias.

The results from the fifth experiment clearly shows that the family of metric's ability to describe a dataset is highly dependent on the database it is applied to. In the results analysis, it was mentioned that certain classes seemed to be well described by the new family of metrics. For a teddy-bear or a crab the five closest shapes turn out to be from the same class, whereas other results suggested that the metric seemed enable to describe certain classes accurately. Good examples of that are the case of the four-limbed animals and humans. Consequently the sixth experiment was realised to further the understanding of how the metrics describe the different classes. It revealed that only 1 class among the 19 appears to be accurately described, namely the teddy-bears class. Indeed for this class both the defined index of coherence and the standard deviation of the distance to the class mean were minimum. This suggests that the class is mapped in a consistent cluster and no other class is superimposed with it. Moreover, only 5 classes have an index of coherence higher than 2.5, which suggests a significant difference between the mapping resulting from the use of the family metric and the classification expected from the database. This results must however be taken with caution, a lot of choices in the way to evaluate this index are arbitrary. Moreover this study is highly dependent on the database. It was also shown that a tight cluster did not necessarily implied a high index of coherence.

An ideal case *i.e.* where the metrics would perform well, is when there is no diversity of compactness amongst the shapes within a class, and if each class have a different representative model of compactness. That is, a case like the teddy-bears class, indeed the class is shown to be well clustered and the index

of coherence suggests that few shapes from other classes are found close to the center of the cluster. That is, the measurements corresponding to the position of the cluster are representative of the class teddy-bear. If a set of metrics was able to obtain such a result for every class of database the classification rate would be the highest.

6.5 Conjectures

The behaviour of the metric when β tends toward -1.5 was described as valuing more the points closest to the shape center of gravity than the points furthest from it. Consequently, if most of the shape is part of fairly compact base the overall compactness measurement will tend to be high. For these values, the metric could be described as the density of the shape around its center of gravity. Whereas the metric seems to value the point furthest from its center more than the closest. Therefore, the metric seems to behave as a measure of surface sphericity. It is satisfying that the least compact shapes from one end of the spectrum are not the most compact from the other end. If that was so, the merit of the family would have been greatly decreased. Indeed, it is aimed to capture different aspects of a shape rather than opposite aspects. Here, on one end of the spectrum the metric focus on how compact the core of the shape is. On the other end, it is evaluating how close the surface of the shapes are from a sphere. These are complementary aspects but not opposite ones.

It is worth noting that these definitions of the metric seem to relate more easily to human perception, but these described behaviours have not been proven.

Consequently, two conjectures are going to be formulated, they aim at describing the behaviour of the metrics in these extreme cases. In the case of β tending toward -1.5 :

Conjecture 1. *For every pair of shapes S and C such that S is an hollowed sphere and C differs from a sphere, there exists a β_0 such that for every $-1.5 < \beta < \beta_0$, $\mathcal{K}_\beta(S) < \mathcal{K}_\beta(C)$.*

In the context hollowed sphere denotes a sphere with a concentric spherical hole. Obviously the radius of the inner sphere because it would make S a perfect sphere. The conjecture in the case of β tending toward ∞ is the following:

Conjecture 2. *For every pair of shapes S and C such that S is an hollowed sphere and C differs from a sphere, there exists a β_0 such that for every $\beta > \beta_0$, $\mathcal{K}_\beta(S) > \mathcal{K}_\beta(C)$.*

Note that it does not contradict the results from Theorem 4 since it only says something about the relative ordering of the shapes. If these conjectures were proven true, it would confirm the previously described behaviour. It would also increase the confidence of the implementation since these conjectures were deduced from the experiments results. In fact if these conjectures could also falsify this work, if they were proven false, since the experimental results would clearly differs from the theoretical basis. A suggestion to begin a proof of these two conjectures is to compare the relative measurements of an hollowed sphere and a sphere having a spherical defect on its surface. A 2D illustration is given Figure 7.

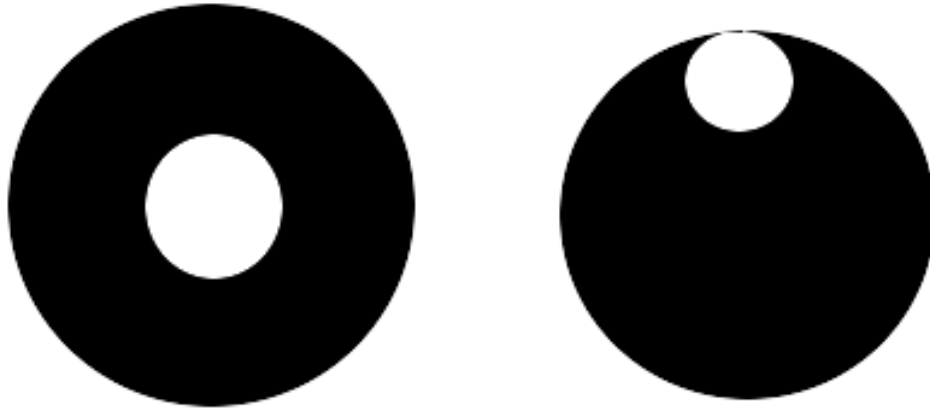


Figure 7: Example of shapes to consider to realise the proof.

6.6 The metrics in a more general context

The seventh experiment investigates how well the new family describes McGill's database when used in combination with other previously defined metrics. The results show that when used to improve the results obtained by using cubeness metrics the merit of the compactness metrics are limited. It would be interesting to evaluate how different the compactness family and the cubeness family are from each other. Indeed, the only conclusion that can be made from the presented work is that the specific case of compactness for $\beta = -1$ and $\beta = 2$ are not redundant with the cubeness for the same value of β . Even though the results are not as clear as one would have expected they still confirm that the new compactness family can be used in combination with other metrics in order to better the results of an application.

7 Conclusion

The work reported in this thesis consisted of the description of a new family of 3D compactness measures, named $\mathcal{K}_\beta(S)$. The metrics are based on a 3D Hu invariant but a tuning parameter β was introduced to be able to modify the metrics behaviour. They were proven to be ranging over the interval $(0, 1]$ for every β . Similarly, for every tuning, $\mathcal{K}_\beta(S) = 1$ is equivalent to S is a sphere. Finally, it is invariant to translation, rotation and scaling. These results are the extension to the whole family of the properties of the compactness measure described in [33]. Moreover the new family was proven to display a similar property as the 2D family of circularity metrics described in [35], namely for any shape S different from a sphere, the compactness measurement of S tends towards 0 when β tends toward ∞ .

The experiments showed that the ordering of the shapes according to their compactness measurements was changing with β and that the classification performance of an application was different for different values of β . These two results prove that the metrics of the family are not redundant.

The experiments also allowed to formulate two conjectures further explaining the metric behaviour as β changes. For every two shapes S and C such that S is an hollowed sphere and C differs from a sphere, there exists a β_0 such that for every $-1.5 < \beta < \beta_0$, $\mathcal{K}_\beta(S) < \mathcal{K}_\beta(C)$. The other being the inverse behaviour, for every two shapes S and C such that S is an hollowed sphere and C differs from a sphere, there exists a β_0 such that for every $\beta > \beta_0$, $\mathcal{K}_\beta(S) > \mathcal{K}_\beta(C)$. These conjectures interpretation is that the metrics will value more the point close to the

center of gravity as β tends toward -1.5 , whereas the point further away will be considered when β tends toward ∞ .

Some experiments investigated how McGill's database was mapped by the family of compactness measures. Thus, it was shown that the teddy-bears class was well described, indeed the results suggest that it forms a cluster and that no other class seem to be close to its center. The ants and airplanes classes however seem to be well clustered by the process but the experiment results suggests that shapes belonging to other classes are located in their clusters. This makes them difficult to model, and reduces the performance of a classification application.

Finally, the new family of metric was used in combination with the family of cubeness metrics defined in [22]. The results shows an improvement of performance that proves that on certain datasets it could be a good choice to use the two families.

A Proof of Theorem 3 (d)

Consider the hollow sphere S_a , for $a \geq 1$, such that

$$S_a = (x, y, z) \in \mathbb{R}^3 | a \leq (x^2 + y^2 + z^2) \leq a + 1.$$

Let S_{p_a} be the sphere of radius a . Then for every β :

$$\begin{aligned} \iiint_{S_a} (x^2 + y^2 + z^2)^\beta dx dy dz &= \iiint_{S_{p_{a+1}}} (x^2 + y^2 + z^2)^\beta dx dy dz \\ &\quad - \iiint_{S_{p_a}} (x^2 + y^2 + z^2)^\beta dx dy dz \\ &= \frac{4\pi}{2\beta + 3} ((a + 1)^{2\beta+3} - a^{2\beta+3}) \end{aligned} \quad (14)$$

$$= \frac{4\pi}{2\beta + 3} a^{2\beta+3} \left(\left(1 + \frac{1}{a}\right)^{2\beta+3} - 1 \right) \quad (15)$$

Note that the volume of S_a is the case where $\beta = 0$. From (14):

$$\begin{aligned} \mu_{0,0,0}(S) &= \frac{4\pi}{3} ((a + 1)^3 - a^3) \\ &= \frac{4\pi}{3} (3a^2 + 3a + 1) \\ &\sim a^2 \end{aligned} \quad (16)$$

Then from (15) and (16), for $\beta \geq 0$:

$$\begin{aligned} \mathcal{K}_\beta(S_a) &= \frac{3}{2\beta + 3} \left(\frac{3}{4\pi} \right)^{2\beta/3} \frac{\mu_{0,0,0}(S)^{(2\beta+3)/3}}{\iiint_S (x^2 + y^2 + z^2)^\beta dx dy dz} \\ &\sim \frac{a^{\frac{2}{3}(2\beta+3)}}{a^{2\beta+3} \left(\left(1 + \frac{1}{a}\right)^{2\beta+3} - 1 \right)} \end{aligned}$$

The Taylor expansion of $(1 + \frac{1}{a})^{2\beta+3}$ and $\theta \in [0; 1]$ leads to:

$$\begin{aligned}
\mathcal{K}_\beta(S_a) &\sim \frac{1}{a^{\frac{1}{3}(2\beta+3)} \left((1 + \frac{1}{a})^{2\beta+3} - 1 \right)} \\
&\sim \frac{1}{a^{\frac{1}{3}(2\beta+3)} \left(1 + (2\beta + 3)\frac{1}{a} (1 + \theta \cdot \frac{1}{a})^{2\beta+2} - 1 \right)} \\
&\sim \frac{1}{a^{\frac{1}{3}(2\beta+3)} \left(\frac{1}{a} (1 + \theta \cdot \frac{1}{a})^{2\beta+2} \right)} \tag{17}
\end{aligned}$$

Note that $(1 + \theta \cdot \frac{1}{a})^{2\beta+2} \geq 1$, then:

$$\frac{1}{a^{\frac{2}{3}\beta} \left((1 + \theta \cdot \frac{1}{a})^{2\beta+2} \right)} \leq \frac{1}{a^{\frac{2}{3}\beta}} \tag{18}$$

And:

$$\lim_{a \rightarrow \infty} \frac{1}{a^{\frac{2}{3}\beta}} = 0 \tag{19}$$

Finally for every $\beta > 0$, from (17), (18), (19)

$$\lim_{a \rightarrow \infty} \mathcal{K}_\beta(S_a) = 0$$

For every $-\frac{3}{2} < \beta < 0$, (17), (18) results are their inverse, and then give:

$$\lim_{a \rightarrow \infty} \mathcal{K}_\beta(S_a) = \lim_{a \rightarrow \infty} a^{\frac{2}{3}\beta} = 0$$

This proof Theorem 3 (d) assessment.

B Implementation of the compactness measure

The function takes the address of a file in “.im” format and a value for the parameter β . It returns the compactness value for the given β .

```
function k = Kbeta(filename, beta)

k=-1;

obj = kuim_load(filename);

vol = getVolume(obj);

mom = getMoment(obj, beta);

if (beta > 0)

    k = 3/(2*beta + 3)*(3/(4*pi))^(2*beta/3)*vol^((2*beta+3)/3)/mom;

elseif (-1.5 < beta && beta < 0)

    k = (2*beta + 3)/3*((4*pi)/3)^(2*beta/3)*mom/vol^((2*beta+3)/3);

end

end

function vol = getVolume(T)

    vol = sum(sum(sum(T)));

end
```



```

function mom = getMoment(T, beta)

mom = 0;

Cx = 0;

Cy = 0;

Cz = 0;

tabx = [0 0.1 0.2 0.3 0.4 0.5 0.6 0.7 0.8 0.9]
taby = [0 0.1 0.2 0.3 0.4 0.5 0.6 0.7 0.8 0.9]
tabz = [0 0.1 0.2 0.3 0.4 0.5 0.6 0.7 0.8 0.9]

for i = 1:size(T,1)
    for j = 1:size(T,2)
        for k = 1:size(T,3)
            if (T(i,j,k) == 1)
                for l = tabx
                    for m = taby
                        for n = tabz
                            Cx = Cx + i + l;
                            Cy = Cy + j + m;
                            Cz = Cz + k + n;
                        end
                    end
                end
            end
        end
    end
end

```

```

end

    end

    end

end

end

nbpt = length(tabx) * length(taby) * length(tabz);

Cx = Cx/((sum(sum(sum(T))))*nbpt);
Cy = Cy/((sum(sum(sum(T))))*nbpt);
Cz = Cz/((sum(sum(sum(T))))*nbpt);

for i = 1:size(T,1)
    for j = 1:size(T,2)
        for k = 1:size(T,3)
            if (T(i,j,k) == 1)
for l = tabx
            for m = taby
                for n = tabz
x = i+l;
y = j+m;
z = k+n;

```

```
mom = mom + ((x-Cx)^2 + (y-Cy)^2 + (z-Cz)^2)^beta/nbpt;  
    end  
end  
end  
    end  
end  
end  
end  
end  
end
```

References

- [1] Benjamin Berkels, Gina Linkmann, and Martin Rumpf. An $SL(2)$ invariant shape median. *Journal of Mathematical Imaging and Vision*, 37(2):85–97, June 2010.
- [2] E. Bribiesca. A measure of compactness for 3D shapes. *Computers & Mathematics with Applications*, 40(10–11):1275–1284, November 2000.
- [3] Ernesto Bribiesca. An easy measure of compactness for 2D and 3D shapes. *Pattern Recognition*, 41(2):543–554, February 2008.
- [4] U. Castellani, M. Cristani, and V. Murino. Statistical 3D shape analysis by local generative descriptors. *IEEE Transactions on Pattern Analysis and Machine Intelligence*, 33(12):2555–2560, 2011.

- [5] Alan R. Dabney and John D. Storey. Optimality driven nearest centroid classification from genomic data. *PLoS ONE*, 2(10):e1002, October 2007.
- [6] Pedro Domingos and Michael Pazzani. On the optimality of the simple bayesian classifier under zero-one loss. *Machine Learning*, 29(2-3):103–130, November 1997.
- [7] A. Elad and R. Kimmel. On bending invariant signatures for surfaces. *IEEE Transactions on Pattern Analysis and Machine Intelligence*, 25(10):1285–1295, 2003.
- [8] Y. Gao, M. Wang, D. Tao, R. Ji, and Q. Dai. 3d object retrieval and recognition with hypergraph analysis. *IEEE Transactions on Image Processing*, 21(9):4290–4303, 2012.
- [9] J. A. Grant, M. A. Gallardo, and B. T. Pickup. A fast method of molecular shape comparison: A simple application of a gaussian description of molecular shape. *Journal of Computational Chemistry*, 17(14):1653–1666, November 1996.
- [10] Tin Kam Ho, J.J. Hull, and S.N. Srihari. Decision combination in multiple classifier systems. *IEEE Transactions on Pattern Analysis and Machine Intelligence*, 16(1):66–75, January 1994.
- [11] Ming-Kuei Hu. Visual pattern recognition by moment invariants. *IRE Transactions on Information Theory*, 8(2):179–187, February 1962.
- [12] Jian Huang, R. Yagel, Vassily Filippov, and Y. Kurzion. An accurate method

- for voxelizing polygon meshes. In *IEEE Symposium on Volume Visualization, 1998*, pages 119–126, October 1998.
- [13] Deok-Soo Kim, Jae-Kwan Kim, Chung-In Won, Chong-Min Kim, Joon Young Park, and Jong Bhak. Sphericity of a protein via the α -complex. *Journal of Molecular Graphics and Modelling*, 28(7):636–649, April 2010.
- [14] Jia-Guu Leu and Limin Chen. Polygonal approximation of 2-d shapes through boundary merging. *Pattern Recognition Letters*, 7(4):231–238, April 1988.
- [15] Ilya Levner. Feature selection and nearest centroid classification for protein mass spectrometry. *BMC Bioinformatics*, 6(1):68, March 2005. PMID: 15788095.
- [16] Zhouhui Lian, A. Godil, and Xianfang Sun. Visual similarity based 3D shape retrieval using bag-of-features. In *Shape Modeling International Conference (SMI), 2010*, pages 25–36, 2010.
- [17] Zhouhui Lian, Afzal Godil, Benjamin Bustos, Mohamed Daoudi, Jeroen Hermans, Shun Kawamura, Yukinori Kurita, Guillaume Lavoué, Hien Van Nguyen, Ryutarou Ohbuchi, Yuki Ohkita, Yuya Ohishi, Fatih Porikli, Martin Reuter, Ivan Sipiran, Dirk Smeets, Paul Suetens, Hedi Tabia, and Dirk Vandermeulen. A comparison of methods for non-rigid 3D shape retrieval. *Pattern Recognition*, 46(1):449–461, January 2013.
- [18] Zhouhui Lian, Afzal Godil, and Jianguo Xiao. Feature-preserved 3D canoni-

- cal form. *International Journal of Computer Vision*, 102(1-3):221–238, March 2013.
- [19] Zhouhui Lian, Paul L. Rosin, and Xianfang Sun. Rectilinearity of 3D meshes. *International Journal of Computer Vision*, 89(2-3):130–151, September 2010.
- [20] S. Marini and M. Spagnuolo. Structural shape prototypes for the automatic classification of 3D objects. *IEEE Computer Graphics and Applications*, 27(4):28–37, 2007.
- [21] Carlos Martinez-Ortiz and Jovisa Zunic. Measuring cubeness of 3D shapes. In *Progress in Pattern Recognition, Image Analysis, Computer Vision, and Applications, Proceedings*, volume 5856, pages 716–723. Springer-Verlag Berlin, Berlin, 2009.
- [22] Carlos Martinez-Ortiz and Joviša Žunić. A family of cubeness measures. *Machine Vision and Applications*, 23(4):751–760, July 2012.
- [23] E. Rahtu, M. Salo, and J. Heikkilä. A new convexity measure based on a probabilistic interpretation of images. *IEEE Transactions on Pattern Analysis and Machine Intelligence*, 28(9):1501–1512, 2006.
- [24] Nicola Ritter and James Cooper. New resolution independent measures of circularity. *Journal of Mathematical Imaging and Vision*, 35(2):117–127, October 2009.

- [25] Paul L. Rosin. Measuring shape: ellipticity, rectangularity, and triangularity. *Machine Vision and Applications*, 14(3):172–184, July 2003.
- [26] Kaleem Siddiqi, Juan Zhang, Diego Macrini, Ali Shokoufandeh, Sylvain Bouix, and Sven Dickinson. Retrieving articulated 3d models using medial surfaces. *Machine Vision and Applications*, 19(4):261–275, July 2008.
- [27] Miloš Stojmenović and Joviša Žunić. Measuring elongation from shape boundary. *Journal of Mathematical Imaging and Vision*, 30(1):73–85, January 2008.
- [28] Federico Sukno, J. L. Waddington, and Paul f Whelan. Rotationally invariant 3D shape contexts using asymmetry patterns. In *GRAPP-International conference on computer graphics theory and applications*, February 2013.
- [29] Jean-Philippe Thirion. The extremal mesh and the understanding of 3D surfaces. *International Journal of Computer Vision*, 19(2):115–128, August 1996.
- [30] Qiong Wang, George M. Garrity, James M. Tiedje, and James R. Cole. Naïve bayesian classifier for rapid assignment of rRNA sequences into the new bacterial taxonomy. *Applied and Environmental Microbiology*, 73(16):5261–5267, August 2007. PMID: 17586664.
- [31] Lei Xie and Philip E. Bourne. A robust and efficient algorithm for the shape description of protein structures and its application in predicting ligand binding sites. *BMC Bioinformatics*, 8(Suppl 4):S9, May 2007. PMID: 17570152.

- [32] Dengsheng Zhang and Guojun Lu. Review of shape representation and description techniques. *Pattern Recognition*, 37(1):1–19, January 2004.
- [33] J. Zunic, K. Hirota, and C. Martinez-Ortiz. Compactness measure for 3D shapes. In *2012 International Conference on Informatics, Electronics Vision (ICIEV)*, pages 1180–1184, 2012.
- [34] J. Zunic, P.L. Rosin, and L. Kopanja. On the orientability of shapes. *IEEE Transactions on Image Processing*, 15(11):3478–3487, 2006.
- [35] Joviša Žunić, Kaoru Hirota, and Paul L. Rosin. A hu-moment invariant as a shape circularity measure. *Pattern Recognition*, 43(1):47–57, January 2010.